

Chemical Reviews

Volume 77, Number 6 December 1977

Circularly Polarized Luminescence Spectroscopy[†]

FREDERICK S. RICHARDSON* and JAMES P. RIEHL

Department of Chemistry, University of Virginia, Charlottesville, Virginia 22901

Received March, 16, 1977 (Revised Manuscript Received June 20, 1977)

Contents

I. Introduction	000
II. Theory	000
A. General Formulation	000
1. Hamiltonian	000
2. Circularly Polarized Luminescence (CPL)	000
3. Magnetic Circularly Polarized Luminescence (MCPL)	000
B. Photoselection and Orientational Relaxation	000
1. General Aspects	000
2. Intensities and Observables	000
C. Dissymmetry Factors (Natural CPL)	000
1. Definition	000
2. Limiting Results	000
3. Experimental Configurations and Excitation Polarizations	000
4. Molecular Transition Vectors	000
D. Comparison of Electronic Rotatory Strengths Obtained from CPL and CD Band Spectra	000
III. Measurement Procedures and Techniques	000
A. General Aspects	000
B. Instrumentation	000
IV. Survey of Applications	000
A. Natural CPL	000
1. Lanthanide Ion Complexes	000
2. Transition Metal Complexes	000
3. Small Organic Molecules	000
4. Biomolecular Systems	000
5. Crystals	000
B. Magnetic CPL	000
1. Transition Metal Ions	000
2. Lanthanide Ions	000
3. Other Systems	000
V. Related Emission Phenomena	000
A. Circular Polarization of Resonance Fluorescence Excited by Circularly Polarized Radiation	000
B. Fluorescence Detected Circular Dichroism (FDCCD)	000
VI. Summary	000
VII. Appendix	000
VIII. References	000

I. Introduction

Chiroptical methods have been used for many years to probe the stereochemical and electronic structural features of mo-

lecular systems. Optical rotation, optical rotatory dispersion (ORD), and circular dichroism (CD) are extremely sensitive probes of molecular stereochemistry in naturally optically active (chiral) systems, and the observables associated with each of these phenomena may be related directly to parameters characteristic of specific electronic structural details.¹ In most cases, the structural information obtainable by these three chiroptical techniques concerns molecular configurational or conformational features characteristic of thermally equilibrated (relaxed) electronic ground states. In principle, one may also acquire structural information about electronic excited states from CD spectra by detailed analyses of band shapes and vibrational structuring within CD bands, but even when sufficiently resolved CD spectra are available, such analyses depend upon rather uncertain theoretical models of spectroscopic vibronic transitions. In practice, then, optical rotation, ORD, and CD (electronic and vibrational) must be considered as probes of molecular (electronic) ground-state structures.

Recently, considerable interest has developed in using the emission analogue of CD to investigate the structural features of the emitting states in chiral luminescent molecular systems. This phenomenon has been variously referred to as circularly polarized emission (CPE) or circularly polarized luminescence (CPL). We shall adopt the latter designation (CPL) in the present review, although it should be understood that in the present context CPE and CPL have identical meanings. Just as CD refers to the differential absorption of left- and right-circularly polarized light by chiral systems, CPL refers to the differential (spontaneous) emission of left- and right-circularly polarized light by chiral luminescent systems. However, whereas the CD observables reflect the chirality of molecular ground states, the CPL observables reflect the chirality of molecular emitting states. CPL, then, provides a probe of configurational and conformational structure in the emitting (or luminescent) states of molecular systems. With regard to molecular structural parameters, the underlying physical principles of CD and CPL are quite similar, and the experimental methods required to measure these two phenomena make similar demands upon instrumentation technology. However, whereas CD has been used extensively over the past 15 years in molecular structure studies, development of CPL spectroscopy has occurred mostly over the past 5 years. Furthermore, whereas commercially available CD instrumentation has reached an advanced state of development and construction (making CD measurements a routine exercise), CPL instrumentation is not yet commercially available and measurements are generally carried out using custom-designed and -constructed apparatus.

[†] This research was supported by the National Science Foundation and by the Camille and Henry Dreyfus Foundation (through a Teacher-Scholar Award to F.R.).

The earliest reported measurements of CPL were by Sa-moilov² who observed CD in the individual (f-f) absorption lines and also circular polarization in the (f-f) emission lines of sodium uranyl acetate crystals at liquid helium temperatures. Brodin and Reznichenko³ repeated these experiments and confirmed the presence of circular polarization in the emission spectrum of crystalline sodium uranyl acetate. Neunhoeffer and Ulrich⁴ observed CPL from the sodium salt of 1,3,5-triphenylpyrazolinesulfonic acid both in the crystalline state and in glycerine solution. These early, isolated observations of CPL did not stimulate much interest in the phenomenon, however, and the results were not subjected to detailed interpretation. The first significant exploitation of CPL as a molecular structure probe can be found in the pioneering studies of Oosterhoff and co-workers at the University of Leiden (The Netherlands). In their initial studies,⁵⁻⁷ Emeis and Oosterhoff irradiated resolved forms (enantiomers) of *trans*- β -hydrindanone, *trans*- β -thiohydrindanone, and Cr(en)₃(ClO₄)₃ in solution with unpolarized light, and measured the relative intensities of the left- and right-circularly polarized components of the emitted light. They defined a *luminescence dissymmetry factor*, $g_{lum} = \Delta I / (I/2) = (I_L - I_R) / (I/2)(I_L + I_R)$, where I_L and I_R denote, respectively, the intensities of the left- and right-circularly polarized components of the emitted light, and compared their measured values of this quantity to the values of the *absorption dissymmetry factor*, $g_{abs} = \Delta\epsilon/\epsilon$, obtained from CD and absorption measurements. In the case of *trans*- β -hydrindanone, they found that the variation of g_{abs} across the absorption band associated with the carbonyl $n \rightarrow \pi^*$ (singlet-singlet) transition was significantly different from the observed variation of g_{lum} across the emission band associated with fluorescence from the $^1n\pi^*$ excited state. From comparisons of absorption (ϵ), circular dichroism ($\Delta\epsilon$), total emission (I), circularly polarized luminescence (ΔI), and linearly polarized luminescence spectra (obtained at room temperature and at 77 K), Emeis and Oosterhoff⁷ were able to deduce specific information about the relative geometries and electronic structural features of the molecular system in its ground state and $^1n\pi^*$ emitting state. This was the first demonstration that CPL could be used to obtain qualitative and quantitative structural information about molecular emitting states.

An early study by Dekkers, Emeis, and Oosterhoff⁸ also demonstrated the possibility of observing CPL from *racemic* mixtures of chiral luminescent systems upon irradiation with circularly polarized exciting light. In this experiment, the sample (racemic mixture of enantiomers) is irradiated with circularly polarized light and the emitted radiation is then analyzed for differential circular polarization. Upon irradiation with, say, left-circularly polarized light, one optical isomer is preferentially excited and the excited-state concentration of this isomer instantaneously exceeds that of its enantiomeric counterpart. If the radiative rate constant exceeds that of racemization within the excited state, then the excited state sample remains (partially) resolved during at least part of the emission process and CPL may be observed. In this type of experiment, the circularly polarized exciting light both photoresolves and optically prepares the sample for the emission event. Scanning the excitation frequency over an absorption band of the sample molecules and monitoring CPL at a fixed emission frequency (that is, measuring excitation spectra) further allows indirect CD measurements on the racemic mixture. This type of experiment has its greatest practical value in studying chiral systems which are difficult or impossible to resolve in their ground states, and for ascertaining whether a compound which does not exhibit CD (or ORD) is a racemic mixture or has a meso structure. Steady-state CPL measurements should be possible if the radiative lifetimes of the emitting states are shorter than the half-life time of racemization. Dekkers et al.⁸ reported CPL measurements on a racemic mixture of *trans*- β -hydrindanone in isoctane irradiated with 317-nm light.

Following Oosterhoff's early experimental studies of CPL phenomena in molecular systems, Steinberg and co-workers at the Weizmann Institute (Israel) and Richardson and co-workers at the University of Virginia (U.S.A.) designed and constructed CPL instrumentation and initiated additional studies in this area.⁹⁻¹¹ Steinberg's work has included studies of small and medium-sized chiral organic systems as well as very extensive applications of CPL spectroscopy to large luminescent biomolecular systems. Richardson's experimental studies have concentrated primarily on chiral luminescent coordination compounds comprised of lanthanide or transition metal ions and organic ligands, and on lanthanide ion/protein complexes. More recently, additional experimental CPL studies from other laboratories have been reported in the literature, and these will be referred to and discussed in section IV of this review. An excellent review of CPL spectroscopy and its application to the study of biomolecular systems has been written by Steinberg.¹²

The early work of Oosterhoff and co-workers included some discussion of the theoretical aspects of molecular CPL. However, the first detailed theoretical analyses of CPL phenomena were published by Snir and Schellman¹³ and by Steinberg and Ehrenberg.¹⁴ Snir and Schellman¹³ considered the effects of excitation photoselection and orientational relaxation (by rotary Brownian motion) on the CPL observables under specific conditions of excitation polarization, excitation-emission geometries, and molecular spectroscopic parameters. Steinberg and Ehrenberg¹⁴ elaborated upon and extended Snir and Schellman's treatment to include consideration of (1) arbitrary excitation-emission geometry, (2) use of polarized exciting radiation, and (3) variable molecular spectroscopic (absorption and emission) parameters. More recently, Riehl and Richardson¹⁵ have proposed a general theory of molecular CPL phenomena.

Just as all materials when placed in a magnetic field exhibit circular dichroism in their absorption regions (called MCD when the field is applied along the direction of light propagation), so should all luminescent materials exhibit CPL in their emission spectra when a magnetic field is applied to them along the direction of emission detection. This emission analogue of MCD has been observed for a number of systems and has been variously referred to as MICE (magnetic induced circular emission), MCE (magnetic circular emission), MCPE (magnetic circularly polarized emission), and MCPL (magnetic circularly polarized luminescence). We shall refer to this phenomenon in the present review as MCPL. MCPL is a rather more extensive topic than natural CPL, and in the present review we shall restrict our consideration of it to aspects of direct chemical structural interest.

The primary emphasis in *natural* CD and CPL studies has been on obtaining stereochemical (configurational and conformational) information on molecular systems, while acquisition of electronic structural information has been of secondary interest. On the other hand, MCD and MCPL studies have been used primarily to investigate electronic structural details of molecules and only secondarily to acquire stereochemical information. The first MCPL studies on molecular systems of direct chemical interest were reported by McCaffery and co-workers¹⁶⁻²⁰ (at the University of Sussex, England), by Richardson and Schatz and co-workers²¹⁻²³ (at the University of Virginia), and by Moreau, Boccara, and Badoz²⁴ (at the Laboratoire d'Optique Physique, France). More recently, Crosby and Hipps²⁵ (at Washington State University) and Schreiner²⁶ (at North Carolina State University) have developed MCPL instrumentation and have been carrying out experimental studies in this area.

The general theory of MCPL and its applications to molecular systems have been treated by Riehl and Richardson in two separate papers^{15,27} and also by Hipps.²⁵

In the present review article we shall proceed by first examining the general theory of CPL and MCPL for molecular systems.

The basic expressions will be developed in a quantum electrodynamic representation and special effects arising from excitation photoselection, reorientational relaxation, excitation polarization, excitation-emission geometry, energy transfer processes, and intramolecular thermal equilibration processes will be treated explicitly. Next we shall discuss measurement procedures and techniques currently in use, and the relationships between experimental observables and theoretical quantities. Finally, the various applications of CPL and MCPL will be surveyed and discussed, and a general assessment of their general utility as spectroscopic structure probes will be offered.

II. Theory

The general quantum theoretical basis of CPL and MCPL (appropriate for molecular systems) will be presented here in a form similar to that found in ref 15 and 27. Although the formalism and methods employed in the present treatment are similar to those presented previously, many details have been eliminated, and the reader is referred to the previous work for a complete account of the basic theory.

A. General Formulation

1. Hamiltonian

The interaction of an electromagnetic field with an ensemble of molecules may be described (to an appropriate level of approximation) by the following Hamiltonian operator (in the coulomb gauge):^{27,28}

$$\begin{aligned} \mathcal{H} = & \sum_{\alpha} [(2m)^{-1}(\mathbf{p}_{\alpha} - ec^{-1}\mathcal{A}_{\alpha})^2 + (2m^2c^2)^{-1}\mathbf{s}_{\alpha} \\ & \cdot \nabla_{\alpha} V \times (\mathbf{p}_{\alpha} - ec^{-1}\mathcal{A}_{\alpha}) - e(mc)^{-1}\mathbf{s}_{\alpha} \cdot \nabla \times \mathcal{A}_{\alpha}] \\ & + \sum_{\alpha < \alpha'} \{e^2(m^2c^2)^{-1}[\mathbf{s}_{\alpha} \cdot \mathbf{s}_{\alpha'} r_{\alpha\alpha'}^{-3} \\ & - 3(\mathbf{s}_{\alpha} \cdot \mathbf{r}_{\alpha\alpha'}) (\mathbf{s}_{\alpha'} \cdot \mathbf{r}_{\alpha\alpha'}) r_{\alpha\alpha'}^{-5}]\} + V + H_{\text{radiation}} \quad (1) \end{aligned}$$

In eq 1 we have assumed that the nuclei of the molecular system are effectively clamped in their equilibrium positions and, thus, the summations run only over the electrons (α, α'). The mass and charge of an electron are denoted respectively by m and e , \mathbf{s}_{α} is the spin operator for electron α , \mathbf{p}_{α} is the linear momentum operator for electron α , and $r_{\alpha\alpha'}$ is an interelectronic distance. V represents the total field-free potential energy of the electrons arising from all electron-electron and electron-nuclei interactions. \mathcal{A}_{α} , the vector potential of the electromagnetic field at the position of electron α , may, in general, be decomposed into time-dependent (radiation) and time-independent (or static) parts:

$$\mathcal{A}_{\alpha} = \mathbf{a}_{\alpha}(t) + \mathbf{A} \quad (2)$$

In what follows, \mathbf{A} will describe a constant (static) externally applied magnetic field (of strength \mathbf{b}_0). In writing eq 1, all terms arising from spin-orbit, spin-field, and spin-spin interactions have been included.

In a series of papers by Power and co-workers,²⁹⁻³¹ canonical transformations have been applied to Hamiltonians of the form given by eq 1 in order to obtain new forms which ensure gauge invariance and in which the microscopic charges and charge densities give rise to an electric polarization \mathcal{P} and a magnetization \mathcal{M} in multipolar form. The specific transformation may be written formally as follows:

$$H = U\mathcal{H}U^{-1} \quad (3)$$

where

$$U = \exp[(-i/\hbar c) \int \mathcal{P}(r) \cdot \mathcal{A}_{\alpha} d^3r] \quad (4)$$

The volume of integration in eq 4 is over the interaction region (cell), and the polarization $\mathcal{P}(r)$ is defined below.

An excellent discussion of canonical transformations and the problems inherent to the selection of gauge as applied to radiation-molecule Hamiltonians has been presented by Wooley.^{32,33} The replacement of the vector potential in favor of the transverse electric and magnetic field operators eliminates gauge problems but may introduce computational difficulties since matrix elements of length operators between inexact wave functions are, in general, origin dependent. In certain calculations, therefore, where the choice of gauge is of little or no consequence, it is often advantageous to use the vector potential representation of the Hamiltonian (as given, for example, in eq 1). In the present treatment, we perform the transformation (eq 3) and employ the Hamiltonian H rather than \mathcal{H} .

The transformed Hamiltonian may be expressed as

$$\begin{aligned} H = & H_{\text{radiation}} + \sum_{\alpha} (2m)^{-1} \mathbf{p}_{\alpha}^2 + V' - \int \mathcal{P} \cdot \mathbf{e} d^3r \\ & - \int \mathcal{M} \cdot \mathbf{B} d^3r + (1/2) \int \int \mathcal{O}_{ij}(r, r') B_j(r) B_j(r') d^3r d^3r' \\ & + 2\pi \int \mathcal{P}^{\perp 2} d^3r \quad (5) \end{aligned}$$

where

$$V' = V + H_{\text{spin-orbit}} + H_{\text{spin-spin}} \quad (6)$$

$$\mathcal{M} = \mathbf{M}(r) + \mathbf{M}_s(r) \quad (7)$$

$$\mathbf{M}_s = \sum_{\alpha} (e/mc) \mathbf{s}_{\alpha} \quad (8)$$

and

$$\mathbf{B} = \mathbf{b}(r, t) + \mathbf{b}_0 \quad (9)$$

\mathbf{e} and \mathbf{b} are the transverse electric and magnetic (radiation) field operators and $\mathcal{O}_{ij}(r, r')$ is the ij component of the diamagnetic tensor field.³⁴ We have assumed for simplicity that the spin-orbit coupling term commutes with the transformation operator U .³⁵

It is convenient when discussing absorption and/or emission of circularly polarized light to define a set of complex polarization operators,^{36,37}

$$\mathbf{d} = \mathcal{P} + i\mathcal{M} \quad (10a)$$

$$\mathbf{d}^{\dagger} = \mathcal{P} - i\mathcal{M} \quad (10b)$$

and a set of complex electromagnetic field operators

$$\mathbf{f} = \mathbf{e} + i\mathbf{b} \quad (11a)$$

$$\mathbf{f}^{\dagger} = \mathbf{e} - i\mathbf{b} \quad (11b)$$

In second-quantized form, \mathbf{e} and \mathbf{b} are given by:

$$\begin{aligned} \mathbf{e} = & i \sum_{\ell, \sigma} (2\pi\hbar\omega_{\ell}/V_q)^{1/2} \hat{\mathbf{e}}_{\ell\sigma} [a_{\ell\sigma} \exp(i\mathbf{k}_{\ell} \cdot \mathbf{r}) \\ & - a_{\ell\sigma}^{\dagger} \exp(-i\mathbf{k}_{\ell} \cdot \mathbf{r})] \quad (12a) \end{aligned}$$

$$\begin{aligned} \mathbf{b} = & -i \sum_{\ell, \sigma} (2\pi\hbar\omega_{\ell}/V_q)^{1/2} (\hat{\mathbf{e}}_{\ell\sigma} \times \hat{\mathbf{k}}_{\ell}) [a_{\ell\sigma} \exp(i\mathbf{k}_{\ell} \cdot \mathbf{r}) \\ & - a_{\ell\sigma}^{\dagger} \exp(-i\mathbf{k}_{\ell} \cdot \mathbf{r})] \quad (12b) \end{aligned}$$

where $a_{\ell\sigma}^{\dagger}$ and $a_{\ell\sigma}$ are respectively creation and annihilation operators for photons of wave vector \mathbf{k}_{ℓ} (frequency ω_{ℓ}) and polarization σ .

In Figure 1 we illustrate a generalized CPL experiment. The detector is positioned in the positive 3-direction and measures the differential intensity of the left- and right-circularly polarized components of the luminescence, as well as the total luminescence intensity. The emitted radiation is described by its polarization properties ($\sigma = 1$ and 2) with unit vectors $\hat{\mathbf{e}}_{\ell 1}$ and $\hat{\mathbf{e}}_{\ell 2}$,

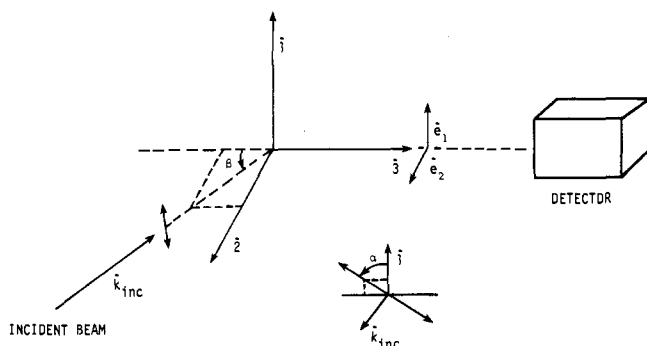


Figure 1. Schematic of a generalized CPL experiment depicting the incident (excitation) radiation, scattering center, emitted radiation, and detector. The coordinates ($\hat{1}$, $\hat{2}$, $\hat{3}$), polarization vectors (\hat{e}_1 and \hat{e}_2), and geometrical parameters (α and β) are defined and discussed in section II of the text.

direction of propagation defined by the unit vector k_ℓ (3-direction), and energy $\hbar\omega_\ell$.

Explicit expressions for f and f^+ are obtained by substitution of eq 12a and 12b into eq 11a and 11b:

$$f(\mathbf{r}) = i \sum_{\ell, \sigma} (8\pi\hbar\omega_\ell/V_Q)^{1/2} [\hat{e}_L a_{\ell L} \exp(i\mathbf{k}_\ell \cdot \mathbf{r}) - \hat{e}_L a_{\ell R}^+ \exp(-i\mathbf{k}_\ell \cdot \mathbf{r})] \quad (13a)$$

$$f^+(\mathbf{r}) = i \sum_{\ell, \sigma} (8\pi\hbar\omega_\ell/V_Q)^{1/2} [\hat{e}_R a_{\ell R} \exp(i\mathbf{k}_\ell \cdot \mathbf{r}) - \hat{e}_R a_{\ell L}^+ \exp(-i\mathbf{k}_\ell \cdot \mathbf{r})] \quad (13b)$$

The unit vectors \hat{e}_R and \hat{e}_L are defined as

$$\hat{e}_R = (2)^{-1/2}(\hat{e}_1 - i\hat{e}_2) \quad (14a)$$

$$\hat{e}_L = (2)^{-1/2}(\hat{e}_1 + i\hat{e}_2) \quad (14b)$$

This is sometimes referred to as the *chemist's* convention and implies that the electric field vector of right-circularly polarized light is viewed as moving in a clockwise manner by an observer situated at the detector and looking back in the negative 3-direction (i.e., looking toward the source). The definitions of the operators $a_{\ell L}$ and $a_{\ell R}$ follow from eq 14a and 14b:

$$a_{\ell L} = (2)^{-1/2}(a_{\ell 1} - ia_{\ell 2}) \quad (15a)$$

$$a_{\ell L}^+ = (2)^{-1/2}(a_{\ell 1}^+ - ia_{\ell 2}^+) \quad (15b)$$

$$a_{\ell R} = (2)^{-1/2}(a_{\ell 1} + ia_{\ell 2}) \quad (15c)$$

$$a_{\ell R}^+ = (2)^{-1/2}(a_{\ell 1}^+ + ia_{\ell 2}^+) \quad (15d)$$

These operators create or annihilate right- (R) or left- (L) circularly polarized photons.

The Hamiltonian (eq 5) may be expressed in terms of the complex polarization and field operators as follows:

$$H = H_0 - (1/2) \int \mathbf{d}(\mathbf{r}) \cdot \mathbf{f}^+(\mathbf{r}) d^3\mathbf{r} - (1/2) \int \mathbf{d}^+(\mathbf{r}) \cdot \mathbf{f}(\mathbf{r}) d^3\mathbf{r} - \int \mathcal{M}(\mathbf{r}) \cdot \mathbf{b}_0 d^3\mathbf{r} \quad (16)$$

where we have discarded, for simplicity, the diamagnetic term and that term involving the square of the transverse polarization field. The zero-order Hamiltonian is given by

$$H_0 = H_{\text{molecule}} + H_{\text{radiation}} \quad (17)$$

where

$$H_{\text{molecule}} = \sum_{\alpha} (2m)^{-1} \mathbf{p}_{\alpha}^2 + V' \quad (18)$$

and

$$H_{\text{radiation}} = (8\pi)^{-1} \int (\mathbf{e}^2 + \mathbf{b}^2) d^3\mathbf{r} \quad (19)$$

Finally, the interaction term may be separated into static

(time-independent) and dynamic (time-dependent) parts as follows:

$$H' = H_1(t) + H_2 \quad (20)$$

where

$$H_1(t) = \int (-1/2) |\mathbf{d} \cdot \mathbf{f}^+ - 1/2| \mathbf{d}^+ \cdot \mathbf{f} d^3\mathbf{r} \quad (21)$$

and

$$H_2 = - \int \mathcal{M} \cdot \mathbf{b}_0 d^3\mathbf{r} \quad (22)$$

2. Circularly Polarized Luminescence (CPL)

The differential spontaneous emission of left- and right-circularly polarized light by chiral molecular systems may be treated by a straightforward application of time-dependent perturbation theory.¹⁵ The differential transition rates that we derive in this section will be expressed in terms of the laboratory coordinate system (1,2,3) shown in Figure 1. The effects of photoselection and orientational relaxation will be discussed in a later section.

The initial (i) and final (f) states of our system will be denoted by

$$|i\rangle = |n; 0\rangle \quad (23)$$

$$|f_L\rangle = |g; \mathbf{k}_\ell \hat{e}_L\rangle \quad (24)$$

$$|f_R\rangle = |g; \mathbf{k}_\ell \hat{e}_R\rangle \quad (25)$$

We assume that the molecule is initially ($t = 0$) in an excited molecular state $|n\rangle$ of energy E_n , and decays (spontaneously) to state $|g\rangle$ of energy E_g with the emission of a left- or right-circularly polarized photon, such that $E_n - E_g \approx \hbar\omega_\ell$. The differential transition rate is given by

$$\Delta W_{if} = W_{ifL} - W_{ifR} \quad (26)$$

where the transition rates are calculated from the "golden rule" expression and eq 21:

$$W_{ifL} = (2\pi/\hbar) |\langle f_L | \int (-1/2) \mathbf{d} \cdot \mathbf{f}^+ d^3\mathbf{r} | i \rangle|^2 \rho_f \quad (27a)$$

$$W_{ifR} = (2\pi/\hbar) |\langle f_R | \int (-1/2) \mathbf{d}^+ \cdot \mathbf{f} d^3\mathbf{r} | i \rangle|^2 \rho_f \quad (27b)$$

Note that only that term in $H_1(t)$ which creates a left-circularly polarized photon contributes to W_{ifL} , and only that term which creates a right-circularly polarized photon contributes to W_{ifR} . The density of final radiation states, ρ_f , is given by:

$$\rho_f = (\omega_\ell^2 V_Q / 8\pi^3 c^3 \hbar) \quad (28)$$

Substituting for f and f^+ from eq 13a and 13b into eq 27a and 27b, and using eq 28, we obtain:

$$W_{ifL} = (\omega_\ell^3 / 2\pi c^3 \hbar) |\hat{e}_R \cdot \mathbf{D}^{gn}|^2 \quad (29a)$$

$$W_{ifR} = (\omega_\ell^3 / 2\pi c^3 \hbar) |\hat{e}_L \cdot \tilde{\mathbf{D}}^{gn}|^2 \quad (29b)$$

where

$$\mathbf{D}^{gn} = \langle g | \int \mathbf{d} \exp(-i\mathbf{k}_\ell \cdot \mathbf{r}) d^3\mathbf{r} | n \rangle \quad (30a)$$

$$\tilde{\mathbf{D}}^{gn} = \langle g | \int \mathbf{d}^+ \exp(-i\mathbf{k}_\ell \cdot \mathbf{r}) d^3\mathbf{r} | n \rangle \quad (30b)$$

The differential transition rate is then given by

$$\Delta W_{if} = (\omega_\ell^3 / 2\pi c^3 \hbar) [\hat{e}_R \cdot \mathbf{D}^{gn} \mathbf{D}^{gn*} \cdot \hat{e}_L - \hat{e}_L \cdot \tilde{\mathbf{D}}^{gn} \tilde{\mathbf{D}}^{gn*} \cdot \hat{e}_R] \quad (31)$$

where (*) denotes complex conjugate, and use has been made of the relation $\hat{e}_L = \hat{e}_R^*$.

The polarization and magnetization may each be expressed as a multipole series.³⁶ For a particular molecule β ,

$$\mathcal{P}_j(\mathbf{r}) = \mu_j(\beta) \delta(\mathbf{r} - \mathbf{R}_\beta) - Q_{jj'} \nabla_{j'} \delta(\mathbf{r} - \mathbf{R}_\beta) + \dots \quad (32)$$

and

$$\mathcal{M}_j(\mathbf{r}) = m_j(\beta) \delta(\mathbf{r} - \mathbf{R}_\beta) - m'_{jj'} \nabla_{j'} \delta(\mathbf{r} - \mathbf{R}_\beta) + \dots \quad (33)$$

where μ_j and $Q_{jj'}$ are, respectively, components of the electric dipole and electric quadrupole moments, and m_j and $m_{j'}$ are, respectively, components of the magnetic dipole and magnetic quadrupole moments. Explicit expressions for the matrix elements \mathbf{D}^{gn} and \mathbf{D}^{gn} may be obtained by substitution of eq 32, 33, 10a, and 10b into eq 30a and 30b. For the j th component we obtain,

$$D_j^{gn} = \mu_j^{gn} + im_j^{gn} - iQ_{jj'}^{gn}(k_\ell)_{j'} \quad (34a)$$

$$\tilde{D}_j^{gn} = \mu_j^{gn} - im_j^{gn} - iQ_{jj'}^{gn}(k_\ell)_{j'} \quad (34b)$$

where we have assumed large (interaction) cell dimensions compared to molecular dimensions to evaluate the integral over cell volume, and all terms in the magnetic quadrupole moment have been dropped. (Note that j' designates the propagation direction of the emitted radiation.) In what follows we shall retain only those terms in the multipolar expansions eq 32 and 33 involving electric and magnetic dipoles and the electric quadrupole.

Substituting eq 34a, 34b, 14a, and 14b into eq 31 we obtain:

$$\Delta W_{if} = K(\omega_\ell^3) [(\mu_2^{gn} Q_{23}^{gn} - \mu_1^{gn} Q_{23}^{gn})k_\ell + i\mu_1^{gn} m_1^{gn} + i\mu_2^{gn} m_2^{gn}] \quad (35)$$

where

$$K(\omega_\ell^3) = (\omega_\ell^3 / \pi c^3 \hbar) \quad (36)$$

and we have assumed that all electric transition moments are pure real and that all magnetic transition moments are pure imaginary. The differential transition rate may be written in the alternative form:

$$\Delta W_{if} = K(\omega_\ell^3) [\text{Re}(\mu_2^{gn} Q_{23}^{gn} - \mu_1^{gn} Q_{23}^{gn})(\omega_\ell/c) - \text{Im}(\mu_1^{gn} m_1^{gn} + \mu_2^{gn} m_2^{gn})] \quad (37)$$

Equation 36 and 37 are appropriate for the case where the emitted light is being observed in the lab 3-direction and the molecular parameters (μ_j^{gn} , m_j^{gn} , and $Q_{jj'}^{gn}$) are defined in the laboratory-fixed 1,2,3-coordinate system.

3. Magnetic Circularly Polarized Luminescence (MCPL)

The circularly polarized luminescence of achiral molecules placed in an externally applied (static) magnetic field may be satisfactorily described by second-order time-dependent perturbation theory in a manner entirely analogous to the first-order treatment presented in the previous section for natural CPL.¹⁵ A more common approach, however, is to first choose eigenfunctions of H_{molecule} (field free) (see eq 18) that are diagonal in $H_2(22)$, and then apply stationary-state perturbation theory to obtain field-dependent perturbed wave functions, followed by a time-dependent perturbation treatment of the molecule-radiation interaction.^{27,28,34} This latter approach is adopted here.

Let $|g\rangle$ and $|n\rangle$ denote, respectively, zero-field ground and excited eigenstates of the field-free electronic Hamiltonian, H_{molecule} . These states may, in general, be degenerate and we shall label the degenerate components as $|g\rangle$ for $|g\rangle$ and as $|n\rangle$ for $|n\rangle$. As stated above, we choose the eigenkets $|g\rangle$ and $|n\rangle$ to diagonalize H_2 . When the magnetic field is "turned-on" the degeneracies will, in general, be lifted and a set of perturbed eigenkets will emerge. These perturbed eigenkets will be labeled $|g'\rangle$ and $|n'\rangle$. To first order in H_2 ,

$$|g'\rangle = |g\rangle + \sum_{k \neq g} |k\rangle \langle k| H_2 |g\rangle / \Delta E_{gk} \quad (38)$$

and

$$|n'\rangle = |n\rangle + \sum_{m \neq n} |m\rangle \langle m| H_2 |n\rangle / \Delta E_{nm} \quad (39)$$

Substitution of eq 22 and 33 into eq 38 and 39 yields to terms linear in b_0 ,

$$|g'\rangle = |g\rangle - \sum_{k \neq g} |k\rangle \langle k| \mathbf{m} |g\rangle \cdot \mathbf{b}_0 / \Delta E_{gk} \quad (40)$$

$$|n'\rangle = |n\rangle - \sum_{m \neq n} |m\rangle \langle m| \mathbf{m} |n\rangle \cdot \mathbf{b}_0 / \Delta E_{nm} \quad (41)$$

The energies of the perturbed states are given by

$$E_{g'} = E_g - \langle g| \mathbf{m} |g\rangle \cdot \mathbf{b}_0 = E_g - \mathbf{m}^{gg} \cdot \mathbf{b}_0 \quad (42)$$

$$E_{n'} = E_n - \langle n| \mathbf{m} |n\rangle \cdot \mathbf{b}_0 = E_n - \mathbf{m}^{nn} \cdot \mathbf{b}_0 \quad (43)$$

The transition rates for the (spontaneous) emission of left- and right-circularly polarized photons may now be calculated as in the previous section (II.A.2). The differential transition rate is given by:

$$\Delta W_{if}^M = W_{if}^M - W_{if}^M = \frac{1}{2} K(\omega_\ell^3) [\hat{\epsilon}_R \cdot \mathbf{D}^{g'n'} \mathbf{D}^{g'n'} \cdot \hat{\epsilon}_L - \hat{\epsilon}_L \cdot \tilde{\mathbf{D}}^{g'n'} \tilde{\mathbf{D}}^{g'n'} \cdot \hat{\epsilon}_R] \quad (44)$$

Substitution of eq 34a, 34b, 10a, and 10b into eq 44 gives the result,

$$\Delta W_{if}^M = -K(\omega_\ell^3) \text{Im} [\mu_2^{n'g'} \mu_1^{g'n'} + m_2^{n'g'} m_1^{g'n'} - i(\omega_\ell/c) (m_1^{n'g'} Q_{13}^{g'n'} + m_2^{n'g'} Q_{23}^{g'n'}) + (\omega_\ell/c)^2 Q_{23}^{n'g'} Q_{13}^{g'n'}] \quad (45)$$

In writing eq 45 we have retained only electric and magnetic dipole terms as well as the electric quadrupole terms. We have also assumed *achiral* luminescent molecular systems and have placed the emission detector in the lab 3-direction.

B. Photoselection and Orientational Relaxation

1. General Aspects

In order to relate the transition rates (calculated above) to observed emission intensities one must take into account the following features which are common to all emission theories for molecules.

(a) The spatial distribution of molecular orientations in the emitting sample will, in general, be anisotropic even if the sample is isotropic in the ground state (as, for example, in a fluid or glassy medium). This anisotropy arises from excitation photoselection. The precise initial distribution created by the exciting light may be calculated from the polarization and direction of the exciting light and the polarization properties of the molecular absorption dipoles (or multipoles).

(b) In considering a fluid sample, the reorientational relaxation of the molecules due to rotary Brownian motion in the time interval between excitation and emission must be suitably described.³⁸⁻⁴⁰

(c) The depletion of the emitting state population due to competing nonradiative relaxation processes must be considered.

We begin our treatment of photoselection and orientational relaxation by defining a function $\Omega(\theta, \phi, t)$ as the probability that the unit vector $\hat{\gamma}$ (which is defined to point along the molecular z axis) is in the direction (θ, ϕ) at time t . The angles (θ, ϕ) are defined with respect to the lab 1,2,3-coordinate axis as shown in Figure 2. From these definitions, it follows that:

$$\Omega(\theta, \phi, t) = \int_0^{2\pi} d\phi_0 \int_0^\pi \sin \theta_0 d\theta_0 \Omega(\theta_0, \phi_0) \times G(\theta_0, \phi_0 | \theta, \phi, t) \quad (46)$$

where $G(\theta_0, \phi_0 | \theta, \phi, t)$ is a function that describes the time evolution of the molecular orientation; $\Omega(\theta_0, \phi_0) = \Omega(\theta, \phi, t = 0)$, and absorption (excitation) takes place at $t = 0$. We further assume that the excitation involves a simple (electric) dipole transition, and that the associated transition dipole vector defines the molecular z axis (i.e., it points in the $\hat{\gamma}$ direction). The initial (t

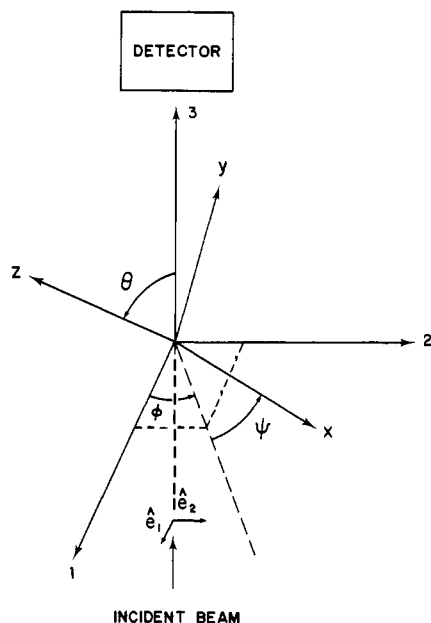


Figure 2. Relationship between the laboratory axes (1, 2, 3) and the molecular axes (X, Y, Z) as defined by the angles of transformation (θ , ϕ , ψ) (see section II.B of text).

= 0) distribution of absorption dipoles (excited molecules) in the sample is calculated from the polarization and direction of the incident (exciting) light beam. Any arbitrarily polarized beam of light may be decomposed into components polarized along the lab axes. For a linearly polarized beam with angles (α, β) (see Figure 1) measured from the lab system, the decomposition may be represented as follows:

$$\hat{e}_1 \cos \alpha + \hat{e}_2 \sin \alpha \cos \beta + \hat{e}_3 \sin \alpha \sin \beta \quad (47)$$

The probability that a molecule will be excited at $t = 0$ is then given by

$$P_{\text{abs}} = \kappa^2 \Omega(\theta_0, \phi_0) = (3/4\pi) \kappa^2 [|\hat{e}_1 \cdot \hat{\gamma}|^2 \cos^2 \alpha + |\hat{e}_2 \cdot \hat{\gamma}|^2 \sin^2 \alpha \cos^2 \beta + |\hat{e}_3 \cdot \hat{\gamma}|^2 \sin^2 \alpha \sin^2 \beta] \quad (48)$$

where κ^2 contains the geometry independent parts of the absorption probability and is, of course, a function of exciting light intensity and the dipole strength of the absorbing transition. Equation 48 may be rewritten as

$$P_{\text{abs}} = \kappa^2 (3/8\pi) [\cos^2 \alpha \sin^2 \theta_0 + \sin^2 \alpha \cos^2 \beta \sin^2 \theta_0 + 2 \sin^2 \alpha \sin^2 \beta \cos^2 \theta_0] \quad (49)$$

or

$$P_{\text{abs}} = \kappa^2 (1/4\pi) [1 - F(\alpha, \beta) P_2(\cos \theta_0)] \quad (50)$$

where F is a geometrical factor defined by

$$F = (1 - 3 \sin^2 \alpha \sin^2 \beta) \quad (51)$$

and $P_2(\cos \theta_0)$ is the Legendre polynomial of order 2. [Note that owing to the specific choice of coordinate system, $\Omega(\theta_0, \phi_0)$, and hence P_{abs} , depends only on the angle θ_0 .]

Equation 46 may be solved by expanding $G(\theta_0, \phi_0 | \theta, \phi, t)$ in terms of spherical harmonics, $Y_{\ell, m}(\theta, \phi)$, with time-dependent coefficients, $C_{\ell, m}(t)$, and by using the appropriate normalization and boundary conditions. The result is easily shown to be:

$$\Omega(\theta, \phi, t) = (1/4\pi) [1 - FC_{2,0}(t) P_2(\cos \theta)] \quad (52)$$

The time-dependent coefficient $C_{2,0}(t)$ [which we shall henceforth abbreviate to $C(t)$] may be viewed as describing the reorientational relaxation in the time-correlation function formalism. Indeed, for parallel transitions in symmetric-top molecules, Gordon⁴¹ has shown that it is this same correlation function that

contributes to the reorientational broadening of the Raman line shape. In time-correlation notation

$$C(t) \equiv C_{2,0}(t) = \langle P_2[\hat{\mu}(0) \cdot \hat{\mu}(t)] \rangle_{\text{ens}} \quad (53)$$

where $\hat{\mu}$ is a unit vector aligned along the transition polarization direction ($\hat{\gamma}$) and the brackets denote an ensemble average.

The time dependence of any quantity, R , that is a function of orientation and which is moving in space is given by

$$R(t, \eta) = R(\eta) \Omega(\eta, t) \quad (54)$$

where $\Omega(\eta, t)$ is given by eq 52. In our applications, $R(\eta)$ will be comprised of molecular matrix elements defined with respect to the lab coordinate system. Equation 54 may be spatially averaged (over all molecular orientations) to obtain the result

$$R(t) = \int R(\eta) \Omega(\eta, t) d\eta = (1/8\pi^2) \int_0^{2\pi} \int_0^{2\pi} \int_0^\pi d\psi d\phi \sin \theta d\theta R(\theta, \phi, \psi) \times [1 - FC(t) P_2(\cos \theta)] \quad (55)$$

where (θ, ϕ, ψ) are the set of Euler angles which take the lab coordinate system (1, 2, 3) into the molecular coordinate system (x, y, z). In the discussion that follows we shall be primarily concerned with systems in which the molecules have random orientations prior to excitation, so that eq 55 is appropriate.

2. Intensities and Observables

The observed differential (spontaneous) emission intensity for natural CPL is related to the differential transition rate, ΔW_{if} , by

$$\Delta I = I_L - I_R = \hbar \omega_\ell N_n \langle \Delta W_{if} \rangle f_{\text{CPL}}(\omega) \quad (56)$$

where N_n is the number of molecules in the emitting state n , $f_{\text{CPL}}(\omega)$ is a normalized line-shape function centered at ω_ℓ , and the brackets denote a *spatial* average appropriate for the orientational distribution of emitting molecules in the sample (see eq 55). Substituting for the differential transition rate from eq 37 into eq 56, we obtain:

$$\Delta I = \hbar \omega_\ell K(\omega_\ell^3) N_n f_{\text{CPL}}(\omega) \langle R^{gn} \rangle \quad (57)$$

where R^{gn} is defined as the *rotatory strength* for the $g \leftarrow n$ transition, and is defined as

$$R^{gn} = i(\mu_x^{gn} m_y^{gn} - \mu_y^{gn} m_x^{gn}) + (\omega_\ell/c)(\mu_z^{gn} Q_{yz}^{gn} - \mu_y^{gn} Q_{xz}^{gn}) \quad (58)$$

Substituting eq 58 into eq 55 and performing the necessary integrations, one obtains the following expression for the time-dependent rotatory strength (expressed in terms of dipole and quadrupole moments referred to the molecular x, y, z -coordinate system):

$$\langle R^{gn}(t) \rangle = i \{ [(2/3) - (1/15) FC(t)] (\mu_x^{gn} m_x^{gn} + \mu_y^{gn} m_y^{gn}) + [(2/3) + (2/15) FC(t)] \mu_z^{gn} m_z^{gn} \} + (1/5) FC(t) K \{ \mu_x^{gn} Q_{yz}^{gn} - \mu_y^{gn} Q_{xz}^{gn} \} \quad (59)$$

Again the brackets $\langle \rangle$ denote a spatial average and it has been assumed that the molecular absorption dipole is pointed in the molecular z direction.

The function $C(t)$, which describes the average random thermal motion of the molecules in the fluid, has been shown to be composed of five exponential decay terms for a completely asymmetric ellipsoidal molecule.⁴² If the molecule has a symmetric ellipsoidal shape, this reduces to three exponentials, and for spherically shaped molecules the motion may be described by a single exponential. Fortunately, most large molecules can be reasonably accurately described as rotating spheres (so-called Einstein spheres) of volume V in a solution of viscosity η . $C(t)$ then has the simple form,

$$C(t) = \exp(-6Dt) \quad (60)$$

where D , the diffusion constant, is given by

$$D = kT/6V\eta \quad (61)$$

Assuming that excitation (at $t = 0$) is directly into the emitting state, n , of the molecule and that the decay of this state follows first-order kinetic processes, then the population of state n at time t is given by

$$N_n = N_n^0 \exp(-t/\tau) \quad (62)$$

where N_n^0 is the state population at $t = 0$ (excitation) and τ is the total "lifetime" of the state. The "lifetime" parameter τ may be expressed as

$$\frac{1}{\tau} = \frac{1}{\tau_{\text{rad}}} + \frac{1}{\tau_q} \quad (63)$$

where $(1/\tau_{\text{rad}})$ is the rate constant for radiative decay and $(1/\tau_q)$ is the rate constant for radiationless decay processes. When excitation is into a molecular state higher in energy than the emitting state n , eq 62 remains valid *only* if relaxation processes leading to population of n are much faster than $(1/\tau)$. In what follows we shall assume that the excited-state manifold of the luminescent molecular system has reached a thermal equilibrium prior to emission and that N_n^0 may be treated as a constant (independent of time).

Substitution of eq 59, 60, and 62 into eq 57 yields the following expression for the time-resolved differential CPL intensity:

$$\begin{aligned} \Delta I(t) = & \hbar\omega_\ell K(\omega_\ell^3) N_n^0 \exp(-t/\tau) f_{\text{CPL}}(\omega) \{ i[(2/3) \\ & - (1/15) F \exp(-6Dt)] [\mu_x^{gn} m_x^{gn} + \mu_y^{gn} m_y^{gn}] \\ & + i[(2/3) + (2/15) F \exp(-6Dt)] \mu_z^{gn} m_z^{gn} \\ & + (1/5) F \exp(-6Dt) k_\ell [\mu_x^{gn} Q_{yz}^{gn} - \mu_y^{gn} Q_{xz}^{gn}] \} \quad (64) \end{aligned}$$

To date, there have been no reported measurements of "time-resolved" CPL, and such measurements would be exceedingly difficult (but not impossible) to perform. All of the reported data have been obtained in the "steady-state" mode. The appropriate expression for a steady-state experiment is obtained by averaging eq 64 over long times:

$$\begin{aligned} \Delta I = & \int_0^\infty \Delta I(t) dt \\ = & \hbar\omega_\ell K(\omega_\ell^3) N_n^0 \tau f_{\text{CPL}}(\omega) \{ i[(2/3) - F/(90D\tau + 15)] \\ & \times (\mu_x^{gn} m_x^{gn} + \mu_y^{gn} m_y^{gn}) + i[(2/3) + 2F/(90D\tau + 15)] \mu_z^{gn} m_z^{gn} \\ & + [F/(30D\tau + 5)] k_\ell (\mu_x^{gn} Q_{yz}^{gn} - \mu_y^{gn} Q_{xz}^{gn}) \} \quad (65) \end{aligned}$$

The measurement of *absolute* emission intensities is very difficult experimentally. Consequently, the usual procedure in CPL studies is to measure ΔI and I ($= I_L + I_R$) in *arbitrary* (or *relative*) intensity units, and to determine the ratio, $g_{\text{lum}} = \Delta I / (I/2)$, in absolute units. The steady-state total luminescence intensity (I) is given by:

$$\begin{aligned} I = & (1/2) \hbar\omega_\ell K(\omega_\ell^3) N_n^0 \tau f_{\text{TL}}(\omega) \{ [(2/3) - F/(90D\tau \\ & + 15)] (|\mu_x^{gn}|^2 + |\mu_y^{gn}|^2) + [(2/3) + 2F/(90D\tau + 15)] |\mu_z^{gn}|^2 \\ & + (\text{higher order terms}) \} \quad (66) \end{aligned}$$

The steady-state luminescence dissymmetry factor, g_{lum} , is then given by:

$$g_{\text{lum}} = \frac{\Delta I}{I/2} = \left[\frac{4if_{\text{CPL}}(\omega)}{f_{\text{TL}}(\omega)} \right] \times \left[\frac{\{ [(2/3) - F/(90D\tau + 15)] (\mu_x^{gn} m_x^{gn} + \mu_y^{gn} m_y^{gn}) + [(2/3) + 2F/(90D\tau + 15)] \mu_z^{gn} m_z^{gn} - i[F/(30D\tau + 5)] k_\ell (\mu_x^{gn} Q_{yz}^{gn} - \mu_y^{gn} Q_{xz}^{gn}) \}}{\{ [(2/3) - F/(90D\tau + 15)] (|\mu_x^{gn}|^2 + |\mu_y^{gn}|^2) + [(2/3) + 2F/(90D\tau + 15)] |\mu_z^{gn}|^2 \}} \right] \quad (67)$$

$f_{\text{TL}}(\omega)$ and $f_{\text{CPL}}(\omega)$ are normalized line-shape functions for total luminescence (TL) and CPL, respectively. In writing eq 67 we have included only the electric dipole contributions to the total luminescence intensity (I). Equation 67 is a general result showing the explicit dependence of g_{lum} upon (a) excitation polarization and excitation-emission geometry (through the factor F), (b) molecular parameters (D , τ , and the transition moment components), and (c) line-shape factors. Recall once again that eq 67 was derived assuming that the absorption dipoles are oriented (polarized) along the molecular z axis.

MCPL (and MCD) spectra are generally analyzed by resolving the differential emission (or absorption) intensity into the so-called Faraday \mathcal{A} , \mathcal{B} , and \mathcal{C} terms.²⁸ The definitions and derivation of these terms in the context of MCPL theory has been given by Riehl and Richardson²⁷ and will not be reproduced here. We present here only the generalized results for the case when the magnetic field induced Zeeman splitting is much less than the line width. In this case, the *steady-state* differential emission intensity is given (to terms linear in b_0) by:

$$\begin{aligned} \Delta I = & (1/2) \hbar\omega_\ell K(\omega_\ell^3) N_{\mathcal{N}}^0 \{ \mathcal{A}(\mathcal{N} \rightarrow \mathcal{G}) f'_{\text{MCPL}}(\omega) / \hbar \\ & + [\mathcal{B}(\mathcal{N} \rightarrow \mathcal{G}) + \mathcal{C}(\mathcal{N} \rightarrow \mathcal{G}) / kT] f_{\text{MCPL}}^0(\omega) \} b_0 \quad (68) \end{aligned}$$

where $f'_{\text{MCPL}}(\omega)$ is the first derivative of the line shape, and \mathcal{N} and \mathcal{G} imply summations over individual Zeeman levels. Explicit expressions for the \mathcal{A} , \mathcal{B} , and \mathcal{C} parameters in the molecular coordinate system are given in the Appendix (VII) of this review article. These expressions differ slightly from those presented in ref 27. These changes were made so that the Faraday parameters used in MCD (absorption) and MCPL (emission) have identical forms. For a detailed derivation of eq 68 and a general treatment of MCPL theory, the reader is referred to ref 27.

C. Dissymmetry Factors (Natural CPL)

1. Definition

Operationally, the luminescence dissymmetry factor, $g_{\text{lum}}(\omega)$, is defined in terms of the observables, $\Delta I(\omega)$ and $I(\omega)$, as follows:

$$g_{\text{lum}}(\omega) = 2\Delta I(\omega) / I(\omega) \quad (69)$$

This quantity has also been called the emission anisotropy factor or the fluorescence anisotropy factor in various papers dealing with CPL phenomena. We prefer the usage of luminescence dissymmetry factor since the quantity is dependent upon molecular chirality (*dissymmetry*) and arises from spontaneous emission (*luminescence*). The term, emission anisotropy, has a well-defined meaning and has found widespread use in linearly polarized luminescence spectroscopy,⁴³ and its use in CPL spectroscopy can be potentially confusing.

Equation 67 expresses g_{lum} in terms of a set of molecular parameters (D , τ , μ^{gn} , m^{gn}), TL and CPL band-shape functions (f_{TL} and f_{CPL}), and an orientation-dependent factor (F) appropriate to the specific photoselection/orientational relaxation model described in section II.B. In this section we examine the behavior of eq 67 under various experimental conditions (as they affect F and D) and for molecules of specific spectroscopic properties. A more detailed analysis of g_{lum} in terms of molecular parameters will be given in section II.D.

2. Limiting Results

The observed CPL and TL intensities and, consequently, g_{lum} have been shown to be dependent, in a precise manner, on the reorientational motion of the emitting molecules. The explicit dependence, which is illustrated in eq 67, is expressed in terms of the product of the two *dynamic* constants, D , the diffusion constant, and τ , the total emission lifetime. Very often in emission experiments it is possible to make the assumption that

TABLE I. Luminescence Dissymmetry Factors Calculated for Photoselected "Frozen" Samples under Several Conditions of Excitation Polarization and Excitation-Emission Geometry^{a,b}

A. Unpolarized Excitation			
	β	F	
1.	0°	1	("head on" excitation)
			$g_{lum} = 4i[f_{CPL}(\omega)/f_{TL}(\omega)] \times$
			$\frac{3\mu_x^{gn}m_x^{gn} + 3\mu_y^{gn}m_y^{gn} + 4\mu_z^{gn}m_z^{gn} - 3ik_\ell(\mu_x^{gn}Q_{yz}^{gn} - \mu_y^{gn}Q_{xz}^{gn})}{3 \mu_x^{gn} ^2 + 3 \mu_y^{gn} ^2 + 4 \mu_z^{gn} ^2}$
2.	90°	-1/2	("right angle" excitation)
			$\frac{7\mu_x^{gn}m_x^{gn} + 7\mu_y^{gn}m_y^{gn} + 6\mu_z^{gn}m_z^{gn} + (3i/2)k_\ell(\mu_x^{gn}Q_{yz}^{gn} - \mu_y^{gn}Q_{xz}^{gn})}{7 \mu_x^{gn} ^2 + 7 \mu_y^{gn} ^2 + 6 \mu_z^{gn} ^2}$
3.	54.74° (or 125.26°)	0	
			$\mu^{gn} \cdot m^{gn} / \mu^{gn} ^2$
B. Linearly Polarized Excitation			
	α	β	F
1.	0°	90°	1 (\perp to \hat{k}_ℓ)
			$\frac{3\mu_x^{gn}m_x^{gn} + 3\mu_y^{gn}m_y^{gn} + 4\mu_z^{gn}m_z^{gn} - 3ik_\ell(\mu_x^{gn}Q_{yz}^{gn} - \mu_y^{gn}Q_{xz}^{gn})}{3 \mu_x^{gn} ^2 + 3 \mu_y^{gn} ^2 + 4 \mu_z^{gn} ^2}$
2.	90°	90°	-2 (\parallel to \hat{k}_ℓ)
			$\frac{2\mu_x^{gn}m_x^{gn} + 2\mu_y^{gn}m_y^{gn} + \mu_z^{gn}m_z^{gn} + ik_\ell(\mu_x^{gn}Q_{yz}^{gn} - \mu_y^{gn}Q_{xz}^{gn})}{2 \mu_x^{gn} ^2 + 2 \mu_y^{gn} ^2 + \mu_z^{gn} ^2}$
3.	35.26° or 144.74°	90°	0
			$\mu^{gn} \cdot m^{gn} / \mu^{gn} ^2$

^a The samples are presumed to be isotropic in their ground states (prior to excitation). ^b The absorption transition dipole (electric) is taken to be oriented along the molecular Z axis.

either (a) the emitting molecules are effectively "frozen" or "locked-in" to their initial ($t = 0$) distribution, or (b) the photo-selected distribution of molecules has "relaxed" (become random) by the time of emission. Case a would be applicable for molecules with a short lifetime and/or a small diffusion constant (slow rotational motion) such that $D\tau \ll 1$. In this case,

$$g_{lum} = \left[\frac{4if_{CPL}(\omega)}{f_{TL}(\omega)} \right] \times \frac{[(10 - F)(\mu_x^{gn}m_x^{gn} + \mu_y^{gn}m_y^{gn}) + (10 + 2F)\mu_z^{gn}m_z^{gn} - 3iFk_\ell(\mu_x^{gn}Q_{yz}^{gn} - \mu_y^{gn}Q_{xz}^{gn})]}{[(10 - F)(|\mu_x^{gn}|^2 + |\mu_y^{gn}|^2) + (10 + 2F)|\mu_z^{gn}|^2]} \quad (70)$$

Examples of this case would be glassy samples or large fluorescent molecules dissolved in viscous solvents. If the emitting molecules are small enough to reorient rapidly and/or have a long lifetime, such that $D\tau \gg 1$, then they would be treated as case b:

$$g_{lum} = \frac{4if_{CPL}(\omega)(\mu_x^{gn}m_x^{gn} + \mu_y^{gn}m_y^{gn} + \mu_z^{gn}m_z^{gn})}{f_{TL}(\omega)(|\mu_x^{gn}|^2 + |\mu_y^{gn}|^2 + |\mu_z^{gn}|^2)} \quad (71)$$

or

$$g_{lum} = \frac{4if_{CPL}(\omega)\mu^{gn} \cdot m^{gn}}{f_{TL}(\omega)|\mu^{gn}|^2} = \frac{4f_{CPL}(\omega)R^{gn}}{f_{TL}(\omega)D^{gn}} \quad (72)$$

Note that in the "relaxed" limit (case b), the terms involving the electric quadrupole moments vanish, and that the result is independent of the geometrical or orientational factor F (as it must be, of course, since the emitting sample is isotropic in this limit).

3. Experimental Configurations and Excitation Polarizations

In the results presented so far we have assumed that the incident beam is linearly polarized (see Figure 1). The factor F may also be used to describe an unpolarized (or natural) excitation source by summing two perpendicular (linear) polarizations. For example, an unpolarized beam whose direction of propagation is along the 2-axis ($\beta = 90^\circ$) may be decomposed into components linearly polarized in the 1- and 3-directions [i.e., $(1/2)^{1/2}(\hat{e}_1$

$+\hat{e}_3)$. F , in this case, is determined by summing the contributions for $\alpha = 0^\circ$ and $\alpha = 90^\circ$:

$$F = \frac{1}{2}(1 - 3 \sin^2 0^\circ \sin^2 90^\circ) + \frac{1}{2}(1 - 3 \sin^2 90^\circ \sin^2 90^\circ) = -\frac{1}{2} \quad (73)$$

It is sometimes desirable to eliminate the effects of photo-selection from the emission spectra or to combine experiments with different excitation-emission geometries and/or excitation polarizations in order to obtain additional molecular information. In this regard, Tinoco et al.⁴⁴ have carefully analyzed the "frozen" limit case for CPL and FDCD (fluorescence detected circular dichroism). They have shown how one can obtain the CPL (or CD) along the direction of the emission (or absorption) transition moment without having to mechanically (or electrically) orient the molecules. It is seen from eq 67 that, if the incident excitation polarization and excitation-emission geometry are chosen so as to make $F = 0$, then g_{lum} reduces to the form of eq 72. The conditions for F to vanish are apparent from its definition (eq 51); for linearly polarized light, these conditions are satisfied by

$$\sin^2 \alpha = 1/(3 \sin^2 \beta) \quad (74)$$

This condition (74) may always be satisfied if $\sin^2 \beta \geq (1/3)$, i.e., $35.26^\circ \leq \beta \leq 144.74^\circ$. A few special cases of interest are presented in Table I. For unpolarized excitation,

$$\frac{1}{2}(1 - 3 \sin^2 \alpha \sin^2 \beta) + \frac{1}{2}(1 - 3 \cos^2 \alpha \sin^2 \beta) = 0 \quad (75)$$

or

$$\sin^2 \beta = 2/3, \beta = 54.74^\circ \text{ or } 125.26^\circ \quad (76)$$

This result was previously derived by Steinberg and Ehrenberg.¹⁴

4. Molecular Transition Vectors

It is, perhaps, important to restate the somewhat obvious result previously derived; namely, that in the limit that the distribution of excited molecules is isotropic about the emission detection direction, the measured differential and total luminescence intensities are entirely independent of the polarization of the excitation beam or the angle between the excitation and

emission directions. As has been illustrated, an isotropic distribution results from either selecting an experimental configuration such that $F = 0$, or selecting a molecular system that completely relaxes (orientationally) in the time between emission and absorption. It should also be apparent that, in this same limit, the measured quantities (ΔI and I) carry no information regarding the angle between the absorption and emission transition vectors. However, the dependence of ΔI and I upon the strength of the absorption transition remains, owing to the functional dependence of N_n on κ^2 .

For a rigid ("frozen") system, the observed intensities (ΔI and I) contain direct molecular information not only on the magnitude and direction of the emission vectors, but also on the magnitude and direction of the absorption vectors, since, in a sense, the emitting molecule has complete memory [$C(t) = 1$] of the excitation event. This feature of emission spectroscopy has been exploited for many years in measurements of linearly polarized fluorescence in order to determine the angle between the absorption and emission transition vectors.^{12,43} These experiments are typically done by freezing the sample in order to ensure a rigid ensemble of emitting systems.

On the molecular level, the very simplest case of an excitation-emission process would be excitation from state $g \rightarrow n$, followed by emission $g \leftarrow n$; that is, the electronic states involved in absorption and emission are the same. The notion that for a particular electronic transition there exists a unique transition direction (or polarization) is, however, not generally true owing to the vibronic nature of the transitions. The polarizations of the transition moment vectors are determined by the initial and final sets of *vibronic* (vibrational and electronic) quantum numbers and not by the electronic quantum numbers alone. Thus, the transition moment vectors associated with different vibronic components of a given electronic transition may have different polarization properties. Polarization direction may vary across the vibronic profile of an electronic absorption or emission band. This is particularly relevant in studies of low-symmetry chiral compounds where few symmetry constraints are placed on the electronic and vibronic state functions. As was pointed out by Steinberg,¹² CPL studies should include the measurement of g_{lum} across an entire emission band. Variations in g_{lum} across an emission band associated with a *particular* electronic transition generally reflect: (a) differences in the vibronic mechanisms contributing to the dipole vs. rotatory strengths; (b) the presence of several different emitting species with dissimilar chirality properties; or (c) changes in the angle between the absorption and emission dipoles on going from one (emission) vibronic component to another across the emission band envelop. These considerations also apply to situations in which the absorption (excitation) is into a high-energy electronic state, and the emitting state is populated by radiationless processes.

If the absorption and emission transition directions are indeed parallel (i.e., $\mu_x^{gn} = \mu_y^{gn} = 0$, in emission), then g_{lum} again reduces to the isotropic (relaxed) limit (eq 72), since, as demonstrated by Snir and Schellman,¹³ the geometrical factors for the dipole strength and rotatory strength are identical and thus cancel.

Additional considerations need be made when the emitting state is populated by radiationless energy transfer between chromophores in large molecules, for example, proteins. This situation is more complicated, since the relative orientation of the chromophores not only affects the intensities through pure geometrical factors, but also affects the efficiency of the energy transfer itself. This is further complicated by the fact that the fixed relative orientation of the chromophores themselves may in some systems be the principal source of chirality in the emission through a dynamic coupling mechanism.¹³

It is anticipated that studies of this type could yield valuable structural information about macromolecules. However, additional theoretical work must be undertaken, and suitable model

experimental systems must be developed and studied in order that the various contributing factors may be analyzed. Of particular importance is a more complete understanding of higher order (than dipole-dipole) multipolar contributions to radiationless energy transfer, and the effects of static and dynamic orientational averaging.

D. Comparison of Electronic Rotatory Strengths Obtained from CPL and CD Band Spectra

In chiroptical spectroscopy, spectra-structure relationships are generally based on obtaining electronic rotatory strengths from the observed CD (or CPL) spectra and then relating the signs and magnitudes of these rotatory strengths to specific stereochemical and electronic structural features of the molecular system. Detailed models of molecular optical activity are designed to calculate electronic rotatory strengths in terms of parameters related directly to stereochemical and electronic structural details. Here we shall consider the rotatory strength associated with a particular molecular electronic transition, $g \rightarrow n$ in absorption and $g \leftarrow n$ in emission. Furthermore, we shall assume an *isotropic* absorbing sample and an *isotropic* emitting sample. Under these conditions, the absorption rotatory strength and the emission rotatory strength are defined (in the electric dipole-magnetic dipole approximation) by:

$$R^a(g \rightarrow n) = \text{Im} \langle g | \mu | n \rangle \cdot \langle n | \mathbf{m} | g \rangle \quad \text{absorption} \quad (77)$$

$$R^e(g \leftarrow n) = \text{Im} \langle g^* | \mu | n^* \rangle \cdot \langle n^* | \mathbf{m} | g^* \rangle \quad \text{emission} \quad (78)$$

where μ and \mathbf{m} are the electric and magnetic dipole operators, respectively. We shall assume thermal equilibration in *both* the ground state (prior to absorption) and the emitting state (prior to emission), so that $|g\rangle$ and $|n\rangle$ are eigenstates of the ground-state electronic Hamiltonian [$H_0(r, Q)$] and $|g^*\rangle$ and $|n^*\rangle$ are eigenstates of the excited state electronic Hamiltonian [$H_0(r, Q^*)$]. The ground-state normal coordinates are denoted by $\{Q\}$, the excited (emitting) state normal coordinates are denoted by $\{Q^*\}$, and the electronic coordinates are denoted collectively by $\{r\}$.

The experimental observable in CD spectroscopy is $\Delta\epsilon(\omega)$, and $R^a(g \rightarrow n)$ may be related to this quantity according to:

$$R^a(g \rightarrow n) = 23.0 \times 10^{-40} \int_{g \rightarrow n} \Delta\epsilon(\omega) d\omega/\omega \quad (79)$$

where the integration is over the frequency interval spanned by the $g \rightarrow n$ absorption band envelop and $R^a(g \rightarrow n)$ is expressed in cgs units ($\text{esu}^2 \text{cm}^2$). The analogous experimental observable in CPL spectroscopy is $\Delta I(\omega)$, and $R^e(g \leftarrow n)$ may be related to this quantity according to:

$$R^e(g \leftarrow n) = C_n \int_{g \leftarrow n} \Delta I(\omega) d\omega/\omega^4 \quad (80)$$

where the integration is over the frequency interval spanned by the $g \leftarrow n$ emission band envelop and (assuming steady-state emission conditions) C_n is a constant given by

$$C_n = \pi c^3 / N_n \quad (81)$$

where N_n is the "steady-state" population of the emitting state n . Equations 79 and 80 are the expressions required for relating the experimental observables, $\Delta\epsilon(\omega)$ and $\Delta I(\omega)$, to the theoretical quantities, $R^a(g \rightarrow n)$ and $R^e(g \leftarrow n)$, under conditions of sample isotropy (in absorption and emission), complete thermal equilibration (in the states $|g\rangle$ and $|n^*\rangle$), and "steady-state" emission observation.

It is obvious from eq 77 and 78 that $R^a(g \rightarrow n) = R^e(g \leftarrow n)$ only when $H_0(r, Q) = H_0(r, Q^*)$. Insofar as $H_0(r, Q)$ and $H_0(r, Q^*)$ reflect molecular conformational (stereochemical) and other geometrical features in the ground state ($|g\rangle$) and emitting state ($|n^*\rangle$), respectively, observed differences in $R^a(g \rightarrow n)$ and $R^e(g \leftarrow n)$

may be traced to differences in molecular structural details in the ground and emitting states. This may be examined in a bit more detail by performing a simple vibronic analysis of $R^a(g \rightarrow n)$ and $R^e(g \leftarrow n)$ within the Born-Oppenheimer (B-O) approximation. Ignoring all "hot-band" vibronic contributions in both absorption and emission ($T = 0$ K), we may write:

$$\begin{aligned} R^a(g \rightarrow n) &= \sum_{\nu} R^a(g0 \rightarrow n\nu) = \sum_{\nu} \text{Im} \langle g0 | \mu | n\nu \rangle \cdot \langle n\nu | \mathbf{m} | g0 \rangle \\ &= \text{Im} \langle 0 | \langle g | \mu | n \rangle_r \cdot \langle n | \mathbf{m} | g \rangle_r | 0 \rangle_Q \\ &= \text{Im} \langle 0 | \mu^{gn} \cdot \mathbf{m}^{ng} | 0 \rangle_Q \quad (82) \end{aligned}$$

and

$$\begin{aligned} R^e(g \leftarrow n) &= \sum_{\nu} R^e(g\nu \leftarrow n0) \\ &= \sum_{\nu} \text{Im} \langle g\nu | \mu | n0^* \rangle \cdot \langle n0^* | \mathbf{m} | g\nu \rangle \\ &= \text{Im} \langle 0^* | \langle g | \mu | n \rangle_r \cdot \langle n | \mathbf{m} | g \rangle_r | 0^* \rangle_{Q^*} \\ &= \text{Im} \langle 0^* | \mu^{gn} \cdot \mathbf{m}^{ng} | 0^* \rangle_{Q^*} \quad (83) \end{aligned}$$

where a subscript r on a bracket denotes integration over electronic coordinates, a subscript Q or Q^* denotes integration over normal coordinate space ($\{Q\}$ or $\{Q^*\}$, respectively), and the absence of a subscript indicates integration over both $\{r\}$ and $\{Q\}$ (or $\{Q^*\}$). The vibrational levels of the ground state are labeled by ν , and the vibrational levels of the excited electronic state (n) are labeled by ν . $|0\rangle$ denotes the ground vibrational level of the ground electronic state and $|0^*\rangle$ denotes the ground vibrational level of the excited electronic state (n). Within the B-O approximation, both $|g\rangle$ and $|n\rangle$ retain nuclear coordinate dependence and so both μ^{gn} and \mathbf{m}^{ng} are also dependent upon nuclear coordinates (expressed as normal coordinates in the present development). The operators, μ and \mathbf{m} , are pure electronic operators since we are considering transitions between two different electronic states (g and n).

From eq 82 and 83, it is clear that $R^a(g \rightarrow n)$ is just the expectation value of $\text{Im}(\mu^{gn} \cdot \mathbf{m}^{ng})$ in the ground vibrational level of the ground electronic state, and $R^e(g \leftarrow n)$ is the expectation value of $\text{Im}(\mu^{gn} \cdot \mathbf{m}^{ng})$ in the ground vibrational level of the excited (emitting) electronic state (n). Setting $\text{Im}(\mu^{gn} \cdot \mathbf{m}^{ng})$ equal to R_{gn} and expanding this quantity in a Taylor series in Q about the equilibrium nuclear geometry of the ground state ($Q = \bar{Q}$), we obtain for $R^a(g \rightarrow n)$:

$$\begin{aligned} R^a(g \rightarrow n) &= R_{gn}(\bar{Q}) + \sum_{\alpha} (\partial^2 R_{gn} / \partial Q_{\alpha}^2)_{\bar{Q}} \langle 0 | Q_{\alpha}^2 | 0 \rangle_Q \\ &+ \dots = R_{gn}(\bar{Q}) + \sum_{\alpha} R''_{gn,\alpha} \langle 0 | Q_{\alpha}^2 | 0 \rangle_Q + \dots \quad (84) \end{aligned}$$

Likewise, expanding R_{gn} in a Taylor series in Q^* (normal coordinates of the emitting state) about the equilibrium nuclear geometry of the excited state ($Q^* = \bar{Q}^*$), we obtain for $R^e(g \leftarrow n)$:

$$\begin{aligned} R^e(g \leftarrow n) &= R_{gn}(\bar{Q}^*) + \sum_{\beta} (\partial^2 R_{gn} / \partial Q_{\beta}^2)_{\bar{Q}^*} \\ &\times \langle 0^* | Q_{\beta}^2 | 0^* \rangle_{Q^*} + \dots \\ &= R_{gn}(\bar{Q}^*) + \sum_{\beta} R''_{gn,\beta} \langle 0^* | Q_{\beta}^2 | 0^* \rangle_{Q^*} + \dots \quad (85) \end{aligned}$$

Clearly, if a molecule has a different geometry and/or symmetry in the ground (g) and emitting (n) states, then $R^a(g \rightarrow n)$ will, in general, differ from $R^e(g \leftarrow n)$. Both $R_{gn}(\bar{Q})$ and $R''_{gn,\alpha}$ (in eq 84) are evaluated at the equilibrium nuclear geometry of the ground state (g), and both $R_{gn}(\bar{Q}^*)$ and $R''_{gn,\beta}$ (in eq 85) are evaluated at the equilibrium nuclear geometry of the emitting state (n).

The possibility of probing ground-state/excited-state structural differences by comparing measured values of $R^a(g \rightarrow n)$ and

$R^e(g \leftarrow n)$ represents one of the very attractive applications of combined CPL/CD studies. Recall, however, that in order to determine $R^e(g \leftarrow n)$ from experimental data one must evaluate the expression given in eq 80. In all the CPL experiments reported to date, ΔI has been measured in arbitrary (rather than absolute) intensity units precluding the determination of R^e values in terms of absolute magnitude. Experimentally, only the signs and relative intensities of ΔI have been measured and only the signs and relative magnitudes of R^e may be determined. On the other hand, luminescence dissymmetry factors, $g_{\text{lum}} = \Delta I / (I/2)$, have been measured and reported in absolute units. Differences observed in the values of g_{lum} and $g_{\text{abs}} (= \Delta \epsilon / \epsilon)$ for a given electronic transition are also expected to be directly related to ground-state/excited-state structural differences in chiral molecular systems.

The total (net) g_{abs} associated with an electronic transition, $g \rightarrow n$, may be expressed as:

$$\begin{aligned} G_{\text{abs}}(g \rightarrow n) &= 4R^a(g \rightarrow n) / D^a(g \rightarrow n) \\ &= \int_{g \rightarrow n} \frac{\Delta \epsilon(\omega)}{\omega} d\omega / \int_{g \rightarrow n} \frac{\epsilon(\omega)}{\omega} d\omega \quad (86) \end{aligned}$$

where $D^a(g \rightarrow n)$ is the dipole strength of the transition and is defined by,

$$D^a(g \rightarrow n) = |\langle g | \mu | n \rangle|^2 \quad (87)$$

The total (net) g_{lum} associated with an electronic transition, $g \leftarrow n$, may be expressed as:

$$\begin{aligned} G_{\text{lum}}(g \leftarrow n) &= 4R^e(g \leftarrow n) / D^e(g \leftarrow n) \\ &= \int_{g \leftarrow n} \frac{\Delta I(\omega)}{\omega^4} d\omega / \int_{g \leftarrow n} \frac{I(\omega)}{\omega^4} d\omega \quad (88) \end{aligned}$$

where

$$D^e(g \leftarrow n) = |\langle g^* | \mu | n^* \rangle|^2 \quad (89)$$

If $\Delta I(\omega)$ and $I(\omega)$ are measured in the same (arbitrary) intensity units, then the absolute values of $(\Delta I / I)$, G_{lum} , and $g_{\text{lum}}(\omega)$ may be determined. Equation 86 and 88 apply only under conditions of sample isotropy (in absorption and emission), complete thermal equilibration (in the ground and emitting states), and "steady-state" emission observation.

At this point it is important to point out that observed differences between $R^a(g \rightarrow n)$ and $R^e(g \leftarrow n)$ or between $G_{\text{abs}}(g \rightarrow n)$ and $G_{\text{lum}}(g \leftarrow n)$ may be attributable to other than static ground-state/excited-state structural differences (i.e., differences in symmetry or in geometrical parameters). Dynamical perturbations such as those arising from vibronic coupling may differ significantly in the molecular ground and emitting states, and this could also be reflected in observed differences between $R^a(g \rightarrow n)$ and $R^e(g \leftarrow n)$ or between $G_{\text{abs}}(g \rightarrow n)$ and $G_{\text{lum}}(g \leftarrow n)$. Furthermore, vibronically induced perturbations upon the dipole strength quantities (D^a and D^e) will, in general, be qualitatively and quantitatively different than those influencing the rotatory strength quantities (R^a and R^e). For this reason, observed differences between G_{abs} and G_{lum} may reflect other than changes in molecular chirality in going from the electronic ground state to the electronic excited (emitting) state.

The most refined and detailed spectra-structure correlations must be based on CPL/CD band-shape analyses or on the evaluation of CPL/CD band fine-structure features (when resolution permits). Differences in CPL and CD band shapes or fine-structure features carry detailed information about relative ground-state/excited-state structural characteristics and about the nature of vibronic perturbations within the ground and excited states. Exploitation of this aspect of comparative CPL/CD studies is nicely demonstrated in an early paper of Ermeis and Oosterhoff⁷ and in a recent study reported by Dekkers and Closs.⁴⁵

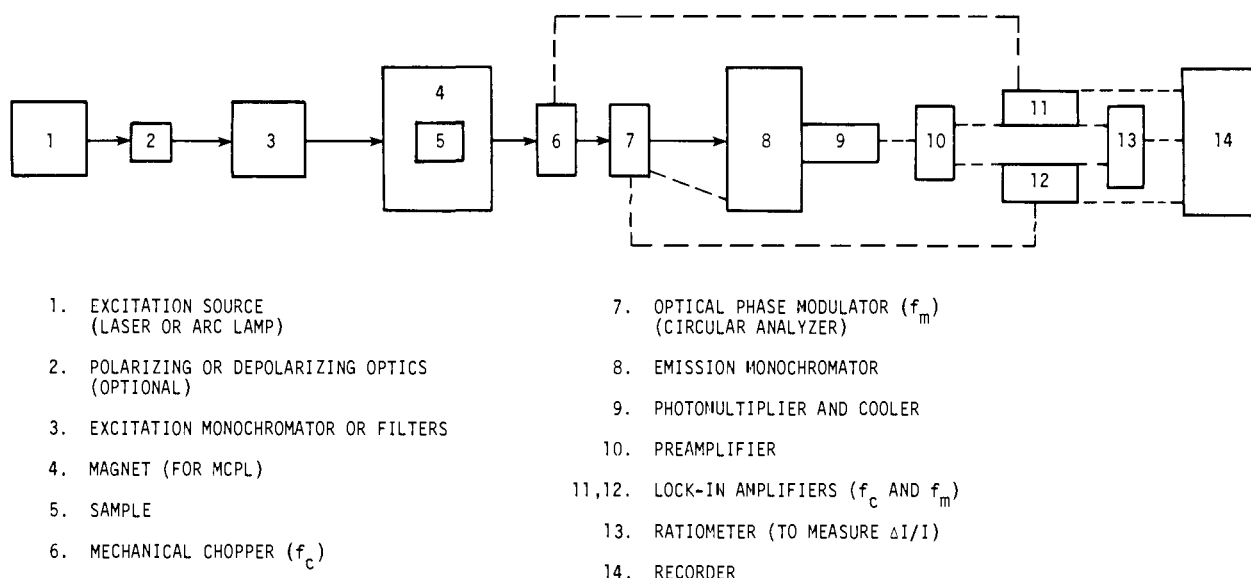


Figure 3. Block diagram depicting the basic components of a CPL spectrophotometer (see section III.B of text).

Equations 86 and 88 yield total (net) values for the absorption and luminescence dissymmetry factors. If the absorption and CD band shapes are identical, then the value of $g_{\text{abs}}(\omega)$ across an absorption/CD band will be constant and equal to $4R^a/D^a$. Likewise, if the total luminescence and CPL band shapes are identical, then the value of $g_{\text{lum}}(\omega)$ across a luminescence/CPL band will be constant and equal to $4R^e/D^e$. That is,

$$g_{\text{lum}}(\omega) = \frac{\Delta I(\omega)}{I(\omega)/2} = \frac{4R^e}{D^e} \frac{f_{\text{CPL}}(\omega)}{f_{\text{TL}}(\omega)} \quad (90)$$

and,

$$g_{\text{lum}} = 4R^e/D^e = G_{\text{lum}} \quad (91)$$

when $f_{\text{CPL}}(\omega) = f_{\text{TL}}(\omega)$ for all ω . Variations in g_{lum} across a total luminescence/CPL band associated with a *particular* electronic transition indicate different vibronic intensity distributions for the total luminescence (I) vs. CPL (ΔI) spectra, and suggest that different vibronic intensity mechanisms contribute to D^e and R^e . Variations in g_{lum} with frequency may also be diagnostic of multiple emitting species in the sample or of simultaneous emission from two (or more) closely spaced electronic excited states.

III. Measurement Procedures and Techniques

A. General Aspects

CPL experiments may be carried out in precisely the same way as any other kind of polarized emission experiment. The only difference between linearly polarized luminescence measurements and circularly polarized luminescence measurements is that, in the latter case, the emitted light is analyzed for its content of left- or right-circularly polarized components, whereas, in the former case, the emitted light is analyzed in terms of linear polarization in one or two (orthogonal) directions.⁴³ The unique feature, then, of any CPL instrumentation is the presence of a *circular analyzer* between the emitting sample and the detector unit. This circular analyzer must be capable of discriminating between left- and right-circularly polarized radiation.

The simplest design for a circular analyzer involves the use of just two optical components: a quarter-wave retardation element followed by a linear polarizer (or analyzer in this case). The quarter-wave retardation element serves to convert circularly polarized light into linearly polarized light. The left- and right-circularly polarized components of the incident light will be linearly polarized in two mutually orthogonal directions. The

linear analyzer then functions to select one or the other of these two linearly polarized components for detection and measurement. To measure ΔI ($=I_L - I_R$), one may take the difference in intensities measured when the linear analyzer is set in the two appropriate mutually orthogonal orientations, or one may keep the orientation of the linear analyzer fixed and measure the difference in intensities produced by (+) or (-) quarter-wave retardation of the incident light. In most instances, it is easier and more convenient to modulate the retardation element between (+) and (-) 90° phase changes than it is to rotate the linear analyzer by $\pm 90^\circ$.

Only two detailed accounts of CPL instrumentation design and construction have appeared in the literature. These were prepared by Steinberg and Gafni⁹ and by Shatwell and McCaffery.²⁰ Additionally, Hipps has given a detailed description of CPL instrumentation design and construction in his Ph.D. dissertation.²⁵ In this review article we shall outline the basic design features of the CPL instrumentation used in our laboratory (University of Virginia). Our instrumentation is similar in design and performance to that used by Steinberg,⁹ by McCaffery,²⁰ and by Hipps.²⁵

B. Instrumentation

A block diagram depicting the basic components of our general-purpose, steady-state CPL instrumentation is given in Figure 3. These components include: (1) excitation source (continuous output), (2) excitation monochromator, (3) excitation beam polarizer, (4) sample cell (or holder), (5) mechanical beam chopper, (6) modulated circular analyzer, (7) emission monochromator, (8) emission detector, (9) phase-sensitive signal amplification electronics, and (10) recorder. In experiments where *unpolarized* excitation light is desired, the excitation beam polarizer may either be removed or be replaced by a depolarizing element (as may be required when a laser excitation source is used or when the output of the excitation monochromator is significantly polarized). MCPL experiments are conducted by placing the emitting sample in a magnetic field whose field direction is aligned parallel to the direction of emission detection.

The mechanical beam chopper (operated at a chopping frequency of $f_c = 13$ Hz) modulates the total emission output of the sample and provides the reference signal for one of the two phase-sensitive lock-in amplifiers in the system. The circular analyzer is comprised of an optical phase modulator (operated at a frequency of $f_m = 50$ kHz) and a stationary linear analyzer.

The optical phase modulator alternately advances and retards the electric vector of the emitted light by 90° which has the effect of converting the circularly polarized components of the light into mutually orthogonal linearly polarized components. The modulated (at f_m) optical signal emerging from the linear analyzer is, then, alternately proportional to the number of left- and right-circularly polarized photons emitted by the sample. The second phase-sensitive, lock-in amplifier in the system is referenced to the $f_m = 50$ kHz frequency of the optical phase modulator.

The electronics of the CPL instrumentation system are designed to amplify the electrical signals supplied by the photomultiplier detector, to discriminate between the signal variables which carry differential circular polarization information and those which are proportional to total emission intensity, and to record any two of the following: (1) CPL intensity (ΔI) in arbitrary units, (2) total luminescence intensity (I) in arbitrary units, and (3) $\Delta I/I$ in absolute units (following instrumentation calibration). The magnitude and phase of the f_m signal carry the CPL intensity and sign information, and the f_c signal carries the total luminescence intensity information.

The dynamically operated quarter-wave retardation element (optical phase modulator) used in our CPL instrumentation (and in Steinberg's,⁹ McCaffery's,²⁰ and Hipps' and Crosby's²⁵) is a photoelastic modulator (PEM) comprised of an isotropic material which is made optically anisotropic upon application of a stress.⁴⁶⁻⁴⁸ The stress is applied periodically at a frequency of 50 kHz, and the stress axis lies in a plane perpendicular to the direction of propagation of the emission beam being analyzed. The voltage of the 50-kHz ac electric field used to introduce the stress determines the phase-shift (or retardation) properties of the PEM. The electronics of the PEM are coupled to the wavelength drive of the emission monochromator to ensure that the PEM introduces phase shifts of $\pm 90^\circ$ (quarter-wave retardation or advancement) on alternate half-cycles of its operation over the entire wavelength range of emission detection and analysis. The linear analyzer positioned behind the PEM is oriented (in a fixed orientation) with its optic axis aligned at $\pm 45^\circ$ to the stress axis of the PEM.

The PEM has found widespread application in ellipsometry,^{46,47} CD,⁴⁹⁻⁵⁵ linear dichroism (LD),⁵⁵ CPL,^{9,20,25} MCD,^{50,56} and polarized fluorescence measurements,⁵⁷ and the reader is referred to the references cited for further discussion of its design, operating, and performance characteristics.

As noted previously, in all of the CPL (and MCPL) experiments reported to date ΔI and I have been measured in arbitrary intensity units. However, in most cases absolute values have been reported for $\Delta I/I$ (the degree of circular polarization). Absolute values of $\Delta I/I$ may be obtained by simply introducing light into the circular analyzer/detector train of the instrument which has a known degree of circular polarization (or ellipticity), and then determining the proportionality constant in the relationship,

$$(\Delta I/I)_{\text{measured}} = C(\Delta I/I)_{\text{known}}$$

C then becomes the instrument calibration factor and may be used to convert measured values of $(\Delta I/I)$ into actual (absolute) values of the degree of circular polarization. This calibration factor will, in general, be wavelength dependent, and it is necessary to know C as a function of (emission) wavelength for doing highly accurate measurements. Perhaps the most accurate and ingenious (but simple) calibration procedure has been developed and discussed by Steinberg and Gafni.⁹

The sensitivity of CPL instrumentation, as determined by how small a value of $\Delta I/I$ may be measured, depends quite critically upon the amount of total emission which can be collected from the sample and (circularly) analyzed. The wide acceptance angle of the PEM unit offers significant advantages in emission collection. For very strong emitters (such as the Mn^{4+} ion in the Cs_2GeF_6 crystalline host), values of $\Delta I/I$ as small as 10^{-6} have

been determined.²¹ In general, the detection limits for $\Delta I/I$ will depend upon: (1) excitation power, (2) radiative quantum efficiencies of emitting species, (3) collection optics and geometry, and (4) other instrumentation factors such as (emission) monochromator efficiency and detector/amplification characteristics.

Time-resolved CPL/MCPL measurements have not yet been reported in the literature, although it is readily apparent from the analysis presented in section II.B that such measurements would be of significant interest and utility.

IV. Survey of Applications

A. Natural CPL

1. Lanthanide Ion Complexes

Many trivalent lanthanide chelate systems are luminescent in solution media at room temperature. Furthermore, when the trivalent lanthanide ion (Ln^{3+}) resides in a chiral ligand environment, its f-f transitions exhibit natural optical activity. The CD/absorption spectra of these transitions are difficult to measure and analyze, however, because the $\Delta\epsilon$ and ϵ values are generally quite small.⁵⁸⁻⁶⁷ Richardson and co-workers have carried out extensive CPL/emission studies on a number of chiral Tb^{3+} and Eu^{3+} complexes in solution media,^{11,68-73} and on a variety of achiral Tb^{3+} and Eu^{3+} chelate systems dissolved in optically active (chiral) solvents.⁷² These studies demonstrated the extreme sensitivity of the CPL observables to metal-ligand binding characteristics, to structural features of the lanthanide ion/ligand complexes, and to chelate-solvent interaction.

CPL spectra have been used to follow the complexation of optically active carboxylic acid ligands with Tb^{3+} and Eu^{3+} in aqueous solution as a function of solution pH.^{11,68,69,73} The ligands examined in these studies included tartaric acid, malic acid, and a wide variety of α -amino acids. Each of these ligands is potentially bidentate or multidentate, and, depending upon denticity, each may bind to the Ln^{3+} ion by single or multiple (bis, tris, or tetrakis) chelations. The mode of metal-ligand binding is expected to be extremely sensitive to solution pH (which determines the availability of ligand donor groups for binding), and the chirality (of the ligand environment) as sensed by the f electrons on the Ln^{3+} ion is determined by the mode of metal-ligand binding. CPL observed for the Ln^{3+} f-f transitions has proved to be a very sensitive probe of the structural characteristics of the ligand environment about the lanthanide ion, and the pH-dependent spectra permit monitoring of structural changes occurring in the ligand environment (due to changes in ligand binding or to alterations in ligand or chelate stereochemistry). Energy transfer between Tb^{3+} and Eu^{3+} ions in aqueous solution with various multidentate optically active carboxylic acids has also been investigated using CPL/emission techniques.^{11,69}

The CPL spectra of chiral tris(β -diketonato)europium(III) chelates in solution media have also been reported.^{70,72} The ligands employed in these studies were 3-trifluoroacetyl-*d*-camphorate (facam) and heptafluoropropylhydroxymethylene-*d*-camphorate (hfc). The optical activity of the f-f transitions in $\text{Eu}(\text{facam})_3$ and $\text{Eu}(\text{hfc})_3$ may arise from configurational dissymmetry due to a chiral distribution of chelate rings about the Eu^{3+} ion, and/or from vicinal interactions between the lanthanide ion and the asymmetric centers in the ligands. The CPL spectra of $\text{Eu}(\text{facam})_3$ and $\text{Eu}(\text{hfc})_3$ were found to be extraordinarily sensitive to the nature of the solvent used, indicating strong solvent perturbations upon the structural details of these chelate systems. Furthermore, the signs and magnitudes of the observed g_{lum} values could be correlated with the relative nucleophilicities (Lewis-base properties) and steric properties of the solvent molecules. The solvents examined in these studies included dimethyl sulfoxide, dimethylformamide, pyridine, saturated ketones, alkyl amines, and alcohols. The sensitivity of the CPL/

emission technique permitted measurements to be made over concentration ranges down to as low as 10^{-3} M in chelate.

CPL spectra on a number of *achiral* tris(β -diketonato)europium(III) chelates dissolved in optically active (chiral) solvents have also been reported. The ligands employed in these studies were: (a) dipivalomethanate (dpm), (b) 2,2-dimethyl-6,6,7,7,8,8,8-heptafluoro-3,5-octanedionate (fod), (c) 1-benzoylmethanate (bzac), (d) dibenzoylmethanate (dbm), and (e) 2,2,6,6-tetramethylheptane-3,5-dionate (tmhd). The chelates, $\text{Eu}(\text{dpm})_3$, $\text{Eu}(\text{fod})_3$, $\text{Eu}(\text{bzac})_3$, $\text{Eu}(\text{dbm})_3$, and $\text{Eu}(\text{tmhd})_3$, are achiral and exhibit no optical activity in achiral solvents. However, when dissolved in an optically active solvent such as α -phenylethylamine, the Eu^{3+} f-f transitions exhibit strong CPL. This induction of CPL in inherently achiral chelate systems by a chiral solvent suggests strong chelate-solvent interactions (perhaps formation of chelate/solvent adducts with well-defined stoichiometries and geometries).

CPL studies have also been reported for chiral $\text{Eu}(\text{facam})_3$ and $\text{Eu}(\text{hfc})_3$ dissolved in the *levo* (*l*) and *dextro* (*d*) forms of α -phenylethylamine.⁷² Substantial differences were observed in the CPL spectra (and in the g_{lum} values) obtained for the *d*(solute)-*d*(solvent) systems vs. the *d*(solute)-*l*(solvent) systems, indicating chiral discrimination (or recognition) in the chelate-(solute)-solvent interactions.

The CPL/emission spectra reported for the terbium(III) complexes in solution media at room temperature were obtained from Tb^{3+} transitions of ${}^7F_J \leftarrow {}^5D_4$ free-ion parentage.^{11,73} The largest $|g_{\text{lum}}|$ values were observed for components of the magnetic-dipole allowed ${}^7F_5 \leftarrow {}^5D_4$ and ${}^7F_3 \leftarrow {}^5D_4$ transitions. In the terbium(III) complexes studied thus far, the 7F_J and 5D_4 free-ion levels are extensively split by the low-symmetry crystal fields created by the ligand environment. For this reason, the sign and splitting patterns observed in the CPL spectra associated with the 7F_6 , 7F_5 , 7F_4 , ${}^7F_3 \leftarrow {}^5D_4$ transitions are exceedingly complex and not amenable to detailed interpretation in the absence of a definitive theoretical model for Ln^{3+} f-f optical activity and absorption/emission intensity.

The CPL/emission spectra reported for chiral europium(III) complexes in solution media at room temperature were obtained from Eu^{3+} transitions of ${}^7F_J \leftarrow {}^5D_0$ (where $J = 0, 1, 2, 3, \text{ or } 4$) free-ion parentage.^{11,69-73} The ${}^7F_2 \leftarrow {}^5D_0$ transition generally exhibits the most intense CPL (ΔI) and total emission (*I*), but the magnetic-dipole allowed ${}^7F_1 \leftarrow {}^5D_0$ transition always produces the largest $|g_{\text{lum}}|$ values. The $|g_{\text{lum}}|$ values for ${}^7F_1 \leftarrow {}^5D_0$ components are generally at least an order of magnitude larger than those observed for ${}^7F_2 \leftarrow {}^5D_0$ components. CPL in the regions of the ${}^7F_3 \leftarrow {}^5D_0$ and ${}^7F_4 \leftarrow {}^5D_0$ transitions is readily observable in most of the cases studied to date,^{69,70,72,73} however, it is somewhat weaker than that observed for the 7F_1 , ${}^7F_2 \leftarrow {}^5D_0$ transitions. The highly forbidden ${}^7F_0 \leftarrow {}^5D_0$ transition exhibits CPL only in a very few systems where the Eu^{3+} ion is presumed to be involved in dimeric or oligomeric species (with possibly strong metal-metal interactions). Both the CPL (ΔI) and total emission (*I*) of this transition are always found to be weak (when observable), and the observed $|g_{\text{lum}}|$ values are $< 10^{-4}$.

From the studies reported to date,⁶⁸⁻⁷³ it appears that CPL/emission spectroscopy is a sensitive and useful technique for probing the structural features and binding characteristics of luminescent Ln^{3+} complexes in solution. The inherent sensitivity of emission measurement techniques permits studies to be conducted at very low concentrations, and the CPL sign and intensity variables are extraordinarily sensitive to stereochemical and electronic structural details of the luminescent systems. However, full exploitation of CPL/emission spectroscopy in structural studies of Ln^{3+} complexes must await development of detailed spectra-structure relationships and an understanding of the mechanisms whereby the Ln^{3+} f-f transitions acquire optical activity in a chiral ligand environment.

2. Transition Metal Complexes

CPL/emission spectra of only one chiral transition metal complex have been reported in the literature. This is rather remarkable in view of the existence of a number of such systems which could be usefully studied by CPL/emission spectroscopy. However, procedures for resolving the optical isomers (enantiomers) of transition metal complexes are not always so straightforward, and the radiative quantum yields of most luminescent transition metal complexes are extremely sensitive to solvent type and temperature. Many transition metal complexes emit strongly only at reduced temperatures (e.g., liquid-nitrogen temperature) in glassy media. Preparation of isotropic, strain-free glasses suitable for CPL experiments is extremely difficult.

Emeis and Oosterhoff^{5,6} measured CPL in the ${}^4A_2 \leftarrow {}^2E$ phosphorescence of $\text{Cr}(\text{en})_3(\text{ClO}_4)$ (*en* = ethylenediamine) dissolved in a 1:2 mixture of water/ethylene glycol at room temperature. They could not obtain a CPL spectrum (ΔI vs. λ), however, because of the weakness of the emission. Using somewhat more sensitive CPL/emission instrumentation, Hilmes, Brittain, and Richardson⁷⁴ succeeded in measuring the CPL/emission spectra of $\text{Cr}(\text{en})_3\text{Cl}_3$ dissolved in a 1:2 water/ethylene glycol solution at room temperature. The $(-)_546\text{-}[\text{Cr}(\text{en})_3\text{Cl}_3]$ isomer exhibited a CPL (ΔI) maximum at $14\,900\text{ cm}^{-1}$ with a g_{lum} value of -0.046 . The single, narrow band appearing in the CPL spectrum is assigned to the spin-forbidden ${}^4A_2 \leftarrow {}^2E$ transition. The corresponding ${}^4A_2 \rightarrow {}^2E$ transition appearing in the CD/absorption spectra of $(-)_546\text{-}[\text{Cr}(\text{en})_3\text{Cl}_3]$ in 1:2 water/ethylene glycol solution has a g_{abs} value of -0.031 at $14\,950\text{ cm}^{-1}$ (the position of the CD maximum).

3. Small Organic Molecules

The class of organic compounds studied most intensively by CPL/emission spectroscopy is that comprised of chiral ketones. The fluorescent level in these systems is the ${}^1n\pi^*$ state. In formaldehyde this state is known to have a somewhat different symmetry (C_s) and geometry from that of the ground electronic state.^{75,76} Pyramidal distortion of the $>\text{C}=\text{O}$ moiety upon going from the ground state to the ${}^1n\pi^*$ excited state is also expected in other, more complicated ketone molecules. Comparative CPL/emission and CD/absorption studies are uniquely suitable as diagnostic probes of such ground-state/excited (emitting)-state structural differences when the molecules are chiral, and when the diagnostic absorption/emission transition is localized near the site of structural change. The $n \rightarrow \pi^*$ transition in chiral ketones satisfies this latter condition completely. Observed differences between CD and CPL band shapes (and origins), as well as between $g_{\text{abs}}(\omega)$ and $g_{\text{lum}}(\omega)$, may be related to ground-state/emitting-state stereochemical differences and/or to different vibronic intensity mechanisms operative in the ground and emitting states.

Emeis and Oosterhoff⁷ have reported a detailed CPL/emission, CD/absorption study of optically active trans- β -hydrindanone, and Dekkers and Closs⁴⁵ have recently reported similar studies on a series of ten additional cyclic monoketone compounds. These studies were all carried out in solution at room temperature. Both relative CPL vs. CD band shapes and relative g_{lum} vs. g_{abs} values were analyzed in terms of ground-state/emitting-state structural differences and differences between absorption and emission vibronic intensity mechanisms. It was concluded that the geometry of the ${}^1n\pi^*$ state in these large ketone systems is significantly distorted with respect to the ground-state equilibrium geometry.

Luk and Richardson¹⁰ have reported the CPL/emission and CD/absorption spectra of the α -diketone, *d*-camphorquinone, in solution at room temperature. The fluorescent level in this compound is a dicarbonyl ${}^1n\pi^*$ state, and the optical activity of the $n \rightarrow \pi^*$ transition can arise from: (a) inherent chirality within

a cisoid dicarbonyl moiety, (b) vicinal perturbations originating with the asymmetric carbon atom in the bicyclic ring system, or (c) both (a) and (b). The g_{abs} value at the CD band maximum (of the lowest energy $n \rightarrow \pi^*$ singlet-singlet transition) was reported to be $\sim -9.0 \times 10^{-3}$, while the corresponding g_{lum} value (measured at the CPL band maximum) was determined to be -1.0×10^{-3} . This order-of-magnitude difference between g_{abs} and g_{lum} was attributed to ground-state/emitting-state (${}^1n\pi^*$) structural differences within the dicarbonyl chromophoric moiety. A detailed analysis of CPL vs. CD band shapes was not attempted.

Brittain and Richardson⁷⁷ have recently reported solvent-induced CPL from the achiral fluorescein molecule. Fluorescein dissolved in optically active α -phenylethylamine (at a 2×10^{-3} M concentration of fluorescein) exhibits CPL over the 500–600-nm region with g_{lum} values ranging from -3×10^{-3} to -6.8×10^{-3} over the broad emission band. This experiment was conducted at room temperature using the 458-nm output of an argon ion laser for excitation. No CD was observed for the fluorescein/ α -phenylethylamine system throughout the 210–500-nm region, and it was concluded that, if solvent-induced CD was present, the $g_{\text{abs}}(\Delta\epsilon/\epsilon)$ value had to be $< 5 \times 10^{-5}$. These results suggest significantly different solute-solvent interactions in the excited (emitting) state vs. the ground state.

Gafni and Steinberg have performed CD/absorption studies and CPL/emission studies on optically active 1,1'-bianthracene-2,2'-dicarboxylic acid in chloroform solution at room temperature.⁷⁸ The luminescent dissymmetry factor, g_{lum} , was measured across the 420–560-nm fluorescence band and was found to be two- to threefold smaller in absolute magnitude than the absorption dissymmetry factor, g_{abs} , measured across the corresponding absorption band (340–430 nm). 1,1'-Bianthracene-2,2'-dicarboxylic does not possess any asymmetric atoms; it is optically active by virtue of inherent chirality about the carbon-carbon single bond which connects the two anthracene moieties in the molecule. Rotation about this single bond is highly restricted owing to steric hindrance, and the molecule may be resolved into two optical isomers in which the two anthracene moieties (and the two carboxyl groups) are in a cisoid ($0^\circ < |\phi| < 90^\circ$), transoid ($90^\circ < |\phi| < 180^\circ$), or perpendicular ($|\phi| = 90^\circ$) arrangement about the C-C single bond ($\phi =$ dihedral angle between the planes of the two anthracene rings). In this system, one may expect the CPL and CD to be extremely sensitive to the equilibrium values of ϕ in the emitting state and ground state, respectively. Using a quantum mechanical extension of the consistent force-field method of conformational analysis, Schlessinger and Warshel⁷⁹ calculated g_{lum} and g_{abs} values as a function of the conformational variable ϕ and compared the calculated values with the experimental data. It was deduced that the difference in dihedral angle between the ground-state and emitting (fluorescent)-state equilibrium conformations is about 20° . In the ground state, the calculated values of ϕ (equilibrium) fall within the range 85 – 100° ; in the excited (emitting) state, the calculated values of ϕ (equilibrium) were reported to be $75 \pm 5^\circ$ and $113 \pm 5^\circ$ (the excited-state conformational energy surface shows two shallow minima, near $\phi = 75^\circ$ and $\phi = 113^\circ$, and the experimental g_{lum} data may be fit using either 75 or 113° for ϕ).

Schlessinger, Gafni, and Steinberg⁸⁰ have reported an exceptionally informative study of the CD/absorption and CPL/emission properties of various cyclic dipeptides containing luminescent aromatic side chains. The electronic transitions localized on the aromatic chromophoric groups of such cyclic dipeptides (diketopiperazines) may acquire optical activity by direct interactions between the aromatic sidechains and chiral features of the diketopiperazine ring (asymmetric centers or chiral ring conformations), or by interactions between two substituted aromatic groups whose relative arrangement in space is chiral. The latter mechanism is operative, of course,

only when two aromatic sidechains are attached to the diketopiperazine system. At room temperature in fluid media, it is expected that considerable conformational space about the diketopiperazine ring is accessible to the aromatic chromophoric groups. It is further expected that, in general, the preferred (lowest energy) regions in this conformational space will differ in the ground and excited states of the molecular systems. Differences in the ground-state and excited-state chiroptical properties will reflect these ground-state vs. excited-state conformational preferences.

In low-viscosity fluid media at room temperature, the lifetimes of the excited aromatic chromophores are long enough to permit partial or complete relaxation of molecular geometry (and conformation) to the emitting state equilibrium geometry before radiative emission occurs. Thus, CPL/emission properties may be correlated with the equilibrium geometry and conformation of the emitting excited state, and CD/absorption spectra may be correlated with the equilibrium structure of the molecular ground state. Schlessinger et al.⁸⁰ studied the CD/absorption and CPL/emission properties of the following cyclic dipeptides in dioxane at room temperature: *cyclo*-(Gly-L-Tyr), *cyclo*-(L-Tyr-L-Tyr), *cyclo*-(L-Trp-L-Phe), *cyclo*-(L-Trp-L-Tyr), *cyclo*-(L-Trp-L-Trp), *cyclo*-(L-Trp-L-Val), and *cyclo*-(L-Trp-D-Val). In each case, excitation was into the lowest energy singlet excited state of the aromatic chromophore, and CPL/emission was measured throughout the fluorescence band associated with the aromatic groups. CD/absorption spectra were measured over the absorption region of the lowest energy singlet-singlet transition in the aromatic chromophores. In the CD results, evidence was found for interactions between the aromatic side chains and the diketopiperazine ring and, in the cases where two aromatic side chains are present, evidence was found for mutual (chiral) interactions between the side chains. However, the most striking result obtained from these studies was the absence of any observable CPL. g_{lum} was measured to be zero to within experimental error (estimated to be $\pm 3 \times 10^{-5}$) in each case. These results suggest drastic differences between the ground-state and fluorescent-state conformational features of the aromatic side chains. In the fluorescent state, the aromatic chromophores do not sense the same chiral environment as they do in the ground state. The same results were obtained when the seven cyclic dipeptide molecules were studied in dimethyl sulfoxide (DMSO) solvent.

Schlessinger et al.⁸⁰ also investigated the CD/absorption and CPL/emission properties of the seven cyclic dipeptide systems (mentioned above) dissolved in highly viscous solvent media comprised of: poly(methyl methacrylate) in chloroform, cellulose acetate in dioxane, or polyoxypropylene in dioxane. The viscosity of these solutions was reported to be so high that they "could hardly flow at room temperature". Under these conditions, it is expected that molecular conformational changes involving the bulky side chains would be very sluggish, and that the associated (conformational relaxation) rate constants would be smaller than the rate constants governing fluorescence. In other words, it is highly likely that the molecular conformation (at least with respect to the bulky side chains) in the fluorescent state will be identical with, or similar to, that characteristic of the equilibrium ground state. The molecule remains "frozen" (conformationally) throughout the excitation/emission sequence of events. These expectations are nicely confirmed by the observation that g_{abs} and g_{lum} are essentially the same when the CD/absorption and CPL/emission measurements are carried out on the highly viscous solutions of the cyclic dipeptides.

Schlessinger et al.⁸⁰ further demonstrated that the rate of rotational (orientational) relaxation of the molecules in the low-viscosity solutions (as monitored by linear polarization of fluorescence measurements) is slower than the conformational relaxation processes responsible for loss of emitting state optical activity (as determined by CPL).

Shindo and Miura⁸¹ have reported CD/absorption and CPL/emission spectra for optically active sodium 1,3,5-triphenyl- Δ^2 -pyrazolinyl sulfate in methanol at room temperature. This system is strongly fluorescent and possesses optical activity by virtue of an asymmetric carbon atom at the 5 position of the pyrazoline ring. The g_{lum} factor was found to be relatively constant ($\sim 4 \times 10^{-4}$) across the 390–560-nm emission band. The maximum value of g_{abs} observed in the corresponding CD/absorption band was determined to be $\sim 16 \times 10^{-4}$.

The number of chiral luminescent organic molecules studied by CPL/emission spectroscopy remains small compared to the large number of such systems which may be usefully investigated by this technique. With the increasing availability of sensitive CPL/emission spectrophotometers, it may be anticipated that many more studies in this area will be carried out in the near future.

4. Biomolecular Systems

Perhaps the most extensive applications of CPL/emission spectroscopy as a structure probe have been in the area of biomolecular structure investigation. In this area, it is generally desirable to study samples in which the concentration of biomolecular species is quite low (e.g., 10^{-3} – 10^{-5} M), making the inherent sensitivity of emission measurement techniques very appealing. Furthermore, most molecular systems of biological interest are inherently chiral, with the degree of chirality being a sensitive indicator of structure or structural change. Steinberg's research group at the Weizmann Institute of Science (Israel) has pioneered the applications of CPL/emission spectroscopy to problems in biomolecular structure evaluation,^{12,82–97} and Martin's and Richardson's research groups at the University of Virginia have made several recent contributions in this area.^{98–102} Additional studies in this area are underway at the University of Calgary (Canada) under the supervision of Professor Rodney Roche.¹⁰³

The CPL/emission investigations carried out by Martin, Richardson, and co-workers^{98–102} have dealt primarily with the use of Tb^{3+} emission as a probe of Ca^{2+} and Mg^{2+} binding sites in proteins. The similarities between Ca^{2+} and Ln^{3+} ions with respect to their coordination chemistries and their physical and chemical properties permit, in many instances, replacement of Ca^{2+} with Ln^{3+} ions in calcium binding proteins without significant alterations in structure. Additionally, in some cases, the enzymatic activity of such proteins is at least partially retained upon replacement of Ca^{2+} with Ln^{3+} ions. Trivalent terbium exhibits a strong luminescence when bound to protein systems, and the intensity and degree of circular polarization of this luminescence appear to depend quite sensitively upon the nature of Tb^{3+} -protein binding and the structural features of the binding sites. Furthermore, the terbium CPL/emission in these systems may be excited by energy transfer from aromatic side chains (of phenylalanine, tyrosine, or tryptophan residues) which are excited directly by near-ultraviolet radiation. Detailed investigations of the excitation/energy-transfer processes leading to terbium CPL/emission afford the opportunity of characterizing the Tb^{3+} binding sites with respect to their proximity to specific aromatic residues in the protein. The circular polarization in the terbium luminescence of these systems is generated by dissymmetric interactions between the f electrons of the bound Tb^{3+} ions and the inherently chiral structure of the protein. Martin, Richardson, and co-workers^{98–102} have reported terbium CPL/emission measurements on 40 different proteins, many but not all of which are known to interact with Ca^{2+} . Thirty-six of these protein/ Tb^{3+} systems show a strong, green emission from terbium upon excitation in the aromatic region (250–300 nm). Circular polarization of terbium emission was observed in nine cases: carp parvalbumin, rabbit skeletal troponin-C, bovine cardiac troponin-C, pronase, porcine elastase, collagenase, bacterial α -

amylase, porcine α -amylase, and thermolysin. The sensitivity levels achieved in these experiments only permitted detection of $|g_{lum}|$ values $> 10^{-3}$. Gafni and Steinberg⁸⁷ have employed terbium CPL/emission to probe the metal binding sites of transferrin and conalbumin. In these systems, g_{lum} values as large as 0.23 were observed in the region of ${}^7F_5 \leftarrow {}^5D_4$ Tb^{3+} emission (530–560 nm) upon excitation with 290–305 nm radiation from a 100-W mercury arc lamp. Epstein¹⁰⁴ has also used terbium CPL/emission in studying the lanthanide binding sites in bovine and porcine trypsin.

Steinberg, Schlessinger, and Gafni^{83,90} have employed acridine dyes as CPL/emission probes of a number of biomolecular systems including: DNA, poly-A, and polyglutamic acid. In these systems, the achiral dye molecules acquire optical activity (CD and CPL) through their binding to the inherently chiral macromolecular structures. Steinberg and co-workers have also studied the CPL/emission properties of a number of other achiral fluorescent probes attached to chiral biomolecular systems. For example, 2-*p*-toluidinylnaphthalene-6-sulfonate (TNS) and the fluorescent anthraniloyl group were used to examine conformational features of chymotrypsin.⁸² In the chymotrypsin–TNS complex, the TNS chromophore is bound at a specific site which is *not* the active site of the enzyme, whereas in the chymotrypsin–anthraniloyl complex the anthraniloyl group is bound at the active site. Dramatic differences between g_{abs} and g_{lum} were observed for the chymotrypsin–TNS complex with g_{lum} being about tenfold smaller than g_{abs} .

The fluorescent analog of NAD^+ , 1, N^6 -ethenoadenine nicotinamide dinucleotide (or ϵNAD), has been used to probe the NAD^+ binding sites in a number of dehydrogenases.^{85,88} From these studies, based on CPL/emission measurements, it was possible to demonstrate that there is a difference in structure between the adenine subsite in rabbit muscle glyceraldehyde 3-phosphate dehydrogenase, on the one hand, and pig heart lactate dehydrogenase, horse liver alcohol dehydrogenase, beef liver glutamate dehydrogenase, and pig heart malate dehydrogenase, on the other hand.

CPL/emission studies of fluorescent dansyl derivatives bound to anti-dansyl antibodies have been reported by Schlessinger, Steinberg, and Pecht.⁸⁶ Sensitivity of the observed CPL to excitation wavelength, to alterations in residues attached to the dansyl group, and to other experimental and structural parameters were correlated to specific features of antibody–hapten interactions. Furthermore, the lack of CD in the 300–400-nm dansyl absorption region for dansyl–anti-dansyl complexes showing strong CPL indicated that a change in the mode of interactions between the chromophore and its binding site takes place upon electronic excitation.

The CPL/emission properties of 1-anilinonaphthalene-8-sulfonate (ANS) bound to bovine serum albumin have been studied by Steinberg, Schlessinger, and Gafni.⁹⁰

Intrinsic protein fluorescence normally occurs from the indole chromophore of tryptophan residues or from the phenol chromophore of tyrosine residues. If both tyrosine and tryptophan residues are present, then the fluorescence is almost always dominated by (or is exclusively due to) tryptophan emission. The intensity and frequency distribution of tryptophan fluorescence from protein systems is quite sensitive to the nature of the environment about the emitting indole moiety (or moieties) in the protein. Furthermore, the linear polarization properties of the tryptophan fluorescence may be related to static or dynamic orientational (or reorientational) characteristics of the emitting chromophore(s). It may be anticipated that the circular polarization of intrinsic protein fluorescence can be used as an additional, and very sensitive, diagnostic probe of the structural features characteristic of the environment of the emitting chromophoric moieties. To this end, Steinberg and co-workers have investigated tryptophanyl (and tyrosyl) CPL/emission in a

number of protein systems.^{89-95,97} Among the systems studied are: azurins and azurin derivatives (derived from *Pseudomonas aeruginosa*),⁹¹ subtilisin types Novo and Carlsberg,⁸⁹ staphylococcal nuclease,⁹⁰ human serum albumin,⁹⁰ chicken pepsinogen,⁹⁰ protein 315 and its fragments (Fab' and Fv),⁹² and various antibody and antibody-ligand systems.^{93-95,97} These studies demonstrated the extreme sensitivity of CPL to protein conformational change, protein-ligand interactions, and protein subunit interactions. In all the cases reported, tryptophan and tyrosine CPL was found to be zero (to within experimental error) for fully reduced and denatured proteins, and the CPL observed for native proteins was found to reflect the effects of secondary and tertiary structure upon the fluorescent aromatic side chains.

Gafni, Hardt, and Steinberg⁹⁶ have also reported CD/absorption and CPL/emission studies on chlorophyll a dimers in solution, subchloroplast particles, and intact chloroplasts. Comparisons between the CD/absorption and CPL/emission results revealed that marked changes in the structure of chlorophyll dimers take place upon electronic excitation.

The application of CPL/emission spectroscopy as a probe of biomolecular structure has been surveyed previously by Steinberg and co-workers.^{12,90} The scope of these applications is enormous, and full exploitation of the CPL technique in the study of biomolecular structure and structural dynamics has yet to be accomplished. CPL arising from intrinsic protein fluorescence has special advantages over CD in probing the (chiral) structural environment of fluorescent aromatic side chains (the indole group of tryptophan, the phenol group of tyrosine, or the phenyl group of phenylalanine). CD observed in the 240-310-nm spectral region of proteins generally reflects "averaged" structural information pertaining to *all* of the tryptophan, tyrosine, phenylalanine, and disulfide moieties present in the system. In most cases, contributions made by specific *kinds* of these chromophoric subunits to the observed CD spectra cannot be resolved or separated out, and contributions made by a *single* chromophoric group can never be satisfactorily assessed except when only one of its kind is present. On the other hand, disulfide moieties are nonfluorescent and hence will never contribute to CPL. Furthermore, phenylalanine residues are fluorescent only in the absence of tryptophan and tyrosine residues, and tyrosine seldom emits in the presence of tryptophan. When fluorescence *does* occur from both tyrosine and tryptophan (as in the subtilisins of type Novo and Carlsberg),⁸⁹ the contributions of tyrosine and tryptophan to the observed CPL may be readily resolved.^{12,89} CPL, then, may be used to probe specific *kinds* of fluorescent aromatic side chains and, in special cases, may be used to probe a specific (single) chromophore. This affords the opportunity of obtaining "local" structure information in complex protein systems.

The CPL associated with extrinsic fluorescent probes attached or bound to biomolecular systems has proved to be an extremely valuable structure tool. Many coenzymes are fluorescent or can be made to luminesce by relatively minor chemical modifications. Luminescent metal ions may be used to probe metal binding sites, and fluorescent ligands (such as dyes) may be found which bind to biomolecular systems in specific ways. Furthermore, enzyme inhibitors are frequently encountered which show a characteristic fluorescence. In each of these cases, the CPL exhibited by the extrinsic fluorescent chromophore is expected to contain detailed information regarding binding and the structural environment of the binding site.

5. Crystals

No reports of natural CPL from optically active crystalline systems have appeared in the literature. However, preliminary investigations of crystalline benzil have been carried out and weak CPL has been observed.¹⁰⁵ Benzil belongs to a small class of molecular systems which are not optically active in solution

but which crystallize into an optically active form. Benzil crystallizes in the trigonal trapezohedral class with a space group $P3_121$ or $P3_221$. The unit cell accommodates three molecules disposed helically about the trigonal axis. The benzil molecule (in the crystalline state) has a skew structure with exact C_2 point-group symmetry. Optical activity in crystalline benzil may derive, then, from both inherent molecular chirality and chirality due to the arrangement of molecules within a unit cell. Crystalline benzil emits at room temperature and exhibits a broad, weak ($|g_{lum}| < 10^{-4}$) CPL in the 490-560-nm region. The emission becomes sharper and more intense at low temperatures, but the crystal appears to undergo a phase transition to a biaxial form near 80 K, making CPL measurements below this temperature impossible. Additional CPL/emission measurements on crystalline benzil down to 80 K are currently in progress (at the University of Virginia).

B. Magnetic CPL

1. Transition Metal Ions

Schatz, Richardson, and co-workers^{21,23} have reported a detailed MCPL/emission study of the ${}^4A_{2g} \leftarrow {}^2E_g$ Mn⁴⁺ transition in crystalline Cs₂GeF₆:Mn⁴⁺. The MCPL/emission measurements were carried out at low temperatures (~5-15 K) and high resolution (spectral band widths < 5 cm⁻¹), and excitation was accomplished using either the 458-nm line or the 488-nm line of an argon ion laser. Cs₂GeF₆:Mn⁴⁺ is cubic, space group O_h ,⁵ with the Ge⁴⁺ (and Mn⁴⁺) ions located at sites of octahedral (O_h) symmetry. Measurements were made with the applied magnetic field (and the emission detection direction) along the [001] (F-Mn-F bond) and the [111] crystallographic axes. Although the Zeeman energy patterns were found to be isotropic, the intensity patterns among Zeeman components in the MCPL/emission spectra were not. This orientation dependence of the intensities associated with components of the ${}^4A_{2g} \leftarrow {}^2E_g$ transition in a magnetic field is in accord with theoretical predictions.¹⁰⁶ The MCPL/emission spectra could be accounted for and interpreted, in large part, in terms of a theoretical analysis based on a crystal-field model and a vibronic intensity model applied to MnF₆²⁻ clusters.

Richardson, Schatz, and co-workers²² have also reported high-resolution, low-temperature MCPL/emission results for Re⁴⁺ (5d³) doped into single crystals of Cs₂ZrCl₆. With 367-nm excitation (from a Xe-Hg arc lamp source), sharp-line MCPL/emission was observed in the 700-740-nm region which was assigned to vibronic components of the $\Gamma_8({}^4A_{2g}) \leftarrow \Gamma_7({}^2T_{2g})$ Re⁴⁺ transition. As λ_{ex} (excitation wavelength) was varied from 367 to 458 nm, emission in the 700-740-nm region was found to diminish (gradually) to zero, but new emission appears in the 740-770-nm region which gradually increases in intensity. At $\lambda_{ex} > 458$ nm, only emission in the 740-770-nm region was observed. Both concentration dependence data and excitation dependence studies suggested that the 740-770-nm emission originates with Re pairs, whereas the 700-740-nm emission features arise entirely from single ion (Re⁴⁺) transitions. The MCPL/emission features observed in the 700-740-nm regions were well accounted for in terms of a crystal-field/vibronic intensity mechanism treatment of octahedral ReCl₆²⁻ clusters. Differences were observed in the MCPL and MCD of specific vibronic components of the intraconfigurational (t_{2g}^3) $\Gamma_8({}^4A_{2g}) \leftarrow \Gamma_7({}^3T_{2g})$ Re⁴⁺ transition. These MCPL vs. MCD differences were attributed to differences in the vibronic mechanisms and phonon coupling in the ground and excited states of the system.

McCaffery and co-workers have reported^{16-19,107-109} several MCPL/emission studies on transition metal ion species. In their initial report,¹⁶ they presented low-temperature (20 K) MCPL/emission spectra of zinc octaethylporphyrin (ZnOEP)

dissolved in a rigid poly(methyl methacrylate) matrix and excited with the 514.5-nm line of an argon ion laser. More recently, they have reported¹⁸ a detailed MCPL/emission study of copper and palladium octaethylporphyrin dissolved in a poly(methyl methacrylate) matrix at 20 K. In this latter study, magnetic moments of the emitting states were obtained, and the results were interpreted in terms of various theoretical treatments of emitting states in diamagnetic and paramagnetic metalloporphyrins. Additionally, a "moments theory" suitable for treating the MCPL results was given.

Another early study of McCaffery and co-workers¹⁷ concerned the MCPL/emission spectra of Cr^{3+} in hexagonal guanidinium aluminum sulfate hexahydrate (GASH). The emission spectra were obtained at liquid helium temperature and excitation was from the 514.5-nm line of an argon ion laser. MCPL/emission was observed over the 14 150–12 800- cm^{-1} region and was assigned to various vibronic and site-group components of the ${}^4\text{A}_2 \leftarrow {}^2\text{E}$ Cr^{3+} transition. Four emission peaks, each with an MCPL A-term, were observed in the ${}^4\text{A}_2 \leftarrow {}^2\text{E}$ origin region (14 150–14 050 cm^{-1}). These features were interpreted in terms of separate emission from the C_{3v} and C_3 Cr^{3+} sites in the hexagonal GASH host lattice. A value of -185 cm^{-1} was deduced for the trigonal-field parameter V . Tentative assignments were offered for the rich vibrational structure observed in the 14 000–12 800- cm^{-1} region. More recently, Shatwell and McCaffery¹⁹ have studied the MCPL/emission spectra of $\text{MgO}:\text{Cr}^{3+}$, and have performed a detailed analysis of the spectra in the ${}^4\text{A}_{2g} \leftarrow {}^2\text{E}_g$ phosphorescence region.

Shatwell and McCaffery^{107,109} have also used MCPL/emission (as well as MCD/absorption) to investigate the ${}^6\text{A}_{1g} \leftrightarrow {}^4\text{T}_{1g}(\text{G})$ transition region of antiferromagnetic MnF_2 .

Moreau et al. have employed MCPL/emission spectroscopy and stress-induced polarized emission spectra to probe Jahn–Teller coupling in the relaxed ${}^1\text{T}_{2g}$ excited state of Ni^{2+} doped into MgO .²⁴ The emission spectra were carried out at 1.3–4.2 K, and 404-nm excitation (${}^3\text{A}_{2g} \rightarrow {}^3\text{T}_{1g}$) from a xenon arc lamp was used. Evidence was obtained for a strong Jahn–Teller coupling of ${}^1\text{T}_{2g}$ with an e_g vibrational mode ($E_{\text{JT}} \approx 515 \text{ cm}^{-1}$).

2. Lanthanide Ions

Although MCPL/emission studies of lanthanide ions and lanthanide ion complexes would appear to hold great promise for eliciting structural information about these complicated systems, only one such study has been reported to date. Richardson, Schwartz, and co-workers¹¹⁰ have measured and analyzed the MCPL/emission spectra of crystalline $\text{Cs}_2\text{NaTbCl}_6$. Low-temperature, high-resolution MCPL/emission spectra were measured throughout the ${}^7\text{F}_6, {}^7\text{F}_5, {}^7\text{F}_4, {}^7\text{F}_3 \leftarrow {}^5\text{D}_4$ transition regions of Tb^{3+} . $\text{Cs}_2\text{NaTbCl}_6$ is cubic with the Tb^{3+} ions located at sites of exact octahedral (O_h) symmetry. A weak-field crystal-field model was used to analyze the MCPL/emission spectra in terms of the crystal-field components of the ${}^7\text{F}_J$ and ${}^5\text{D}_4$ free-ion states. Using the transition energies and A/D ratios (where A is the Faraday A-term and D is the dipole strength) calculated according to this model for the magnetic-dipole allowed transitions, a complete set of assignments was possible in the ${}^7\text{F}_5, {}^7\text{F}_3 \leftarrow {}^5\text{D}_4$ transition regions and additional assignments were made in the ${}^7\text{F}_6, {}^7\text{F}_4 \leftarrow {}^5\text{D}_4$ transition regions. The $\Delta J = \text{odd}$ (${}^7\text{F}_5, {}^7\text{F}_3 \leftarrow {}^5\text{D}_4$) emission spectra exhibited only (0–0) magnetic-dipole lines, whereas the $\Delta J = \text{even}$ (${}^7\text{F}_6, {}^7\text{F}_4 \leftarrow {}^5\text{D}_4$) emission spectra exhibited both magnetic-dipole lines and phonon-assisted electric-dipole lines.

A number of additional MCPL/emission studies on $\text{Cs}_2\text{NaLnCl}_6$ ($\text{Ln} = \text{trivalent lanthanide ion}$) systems have been carried out or are underway, in our laboratory at the University of Virginia, but the data obtained from these studies have not yet been analyzed and reported.¹¹¹ Preliminary MCPL/emission data have also been

acquired on a series of tris(β -diketonate)lanthanide(III) chelates in solution media.¹¹²

3. Other Systems

Marrone and Kabler¹¹³ have observed strong magnetic-field-induced circular polarization in many of the intrinsic recombination (emissive) transitions from a number of alkali halide crystals. In these experiments, the luminescence was excited by 50-kV x-rays and MCPL was measured as a function of magnetic field strength and sample temperature. Excited (emitting) state magnetic moments were determined from the MCPL data, and it was concluded that the observed luminescence originates in triplet states of self-trapped excitons.

Schatz and co-workers (at the University of Virginia) have initiated MCPL/emission studies on luminescent species trapped in rare gas matrices at low temperatures. Preliminary results have been obtained on XeF and KrF (trapped in solid argon and neon matrices) and on Cl_2 (trapped in a solid argon matrix). These emission studies coupled with MCD/absorption measurements show great promise for elucidating the ground-state and emitting-state structural features of such systems.

In a study of predissociation effects in the $\text{B}^3\Pi_{0+u}$ state of molecular iodine, Vigue et al.¹¹⁴ observed magnetic-field-induced circular polarization in the emission spectrum of this state. In these experiments, fluorescence was excited by linearly polarized radiation from a laser source and the emission was observed in the direction of the applied magnetic field. Circular polarization ($I_L - I_R$) of opposite signs was observed for the R and P rotational lines in the fluorescence spectrum. Furthermore, separate lifetime measurements on I_L emission and I_R emission showed that the left- and right-circularly polarized components in the emission had different lifetimes, and that the lifetimes and lifetime differences (between I_L and I_R) were field dependent. They concluded that the circular polarization observed in the emission is a lifetime effect induced by the applied magnetic field. It was postulated that the magnetic field influences the relaxation rates of the $+M$ and $-M$ Zeeman sublevels of the emitting state differently, and that the stationary-state populations of these levels will, consequently, be different. This leads to a net orientation of the emitting state with respect to the magnetic field and to a nonzero ($I_L - I_R$) difference. The influence of the magnetic field upon the relative relaxation rates of the $+M$ and $-M$ Zeeman sublevels was presumed to arise as a direct consequence of interference between magnetic and natural predissociation of the $\text{B}^3\Pi_{0+u}$ state of molecular iodine.

V. Related Emission Phenomena

A. Circular Polarization of Resonance Fluorescence Excited by Circularly Polarized Radiation

The major theme of this review is circular polarization of molecular luminescence arising either from inherent molecular chirality (natural CPL) or from the application of a magnetic field aligned parallel to the direction of emission detection (MCPL). In our theoretical treatment of CPL and MCPL (see section II), we assumed that excitation was effected via electric-dipole absorption processes. The angular momentum properties of the absorbing states were neglected, and the transfer of angular momentum between a circularly polarized excitation beam and the molecule during an absorption event was presumed to have no influence on the CPL and MCPL properties of the emitting system. This treatment is entirely satisfactory under conditions of thermal equilibrium within the molecular excited-state manifold prior to emission, and will usually be satisfactory for representing *non-resonance* emission properties. Under these conditions, the emitting (luminescent) state of the molecular

system has no "memory" of the angular momentum properties of the exciting radiation. However, when resonance fluorescence of molecular systems is excited by circularly polarized radiation under conditions leading to nonthermal distributions of excited (emitting) states, the theory presented in section II of this review is no longer adequate. In this case, the emission may be (partially or entirely) circularly polarized even for achiral molecules in the absence of any externally applied fields.

The origins of circular polarization in the resonance fluorescence of achiral molecules (in the absence of externally applied fields) is not difficult to understand. Circularly polarized exciting radiation will selectively excite rotational levels of the molecular excited states which have well-defined angular momentum (M_J) quantum numbers. In the absence of complete thermal equilibration among the rotational levels of the excited state prior to emission (i.e., complete orientational relaxation of the molecules), the emission will be dominated by those M_J levels populated by direct excitation. Only those M_J levels having angular momenta equal to that of the exciting radiation are excited, and it is these which will dominate the emission. The net angular momentum (and, therefore, circular polarization) of the emitted photon flux will be identical in sign with that of the exciting photon beam. The degree of circular polarization in the emission, $C = (I_L - I_R)/(I_L + I_R)$, will reflect the extent to which thermal relaxation and reorientational motion occurs prior to emission. In effect then, C is a measure of the relative populations of the M_J levels in the molecular emitting states and may be related to various elastic and rotationally inelastic collisional processes occurring in the sample.

Detailed consideration of circularly polarized resonance fluorescence from molecules excited with circularly polarized light lies outside the scope of this review article. The reader is referred to Feofilov¹¹⁵ and to several recent papers by McCaffery and co-workers¹¹⁶⁻¹¹⁸ for more detailed discussions of this phenomenon and its applications to the study of molecular structure and dynamics. The recent work of McCaffery and co-workers¹¹⁶⁻¹¹⁸ on circularly polarized emission from molecular iodine demonstrates the great potential of this technique as a spectroscopic probe of molecular excited-state dynamics. The circular polarization of the rotationally resolved emission from diatomic molecules contains much information on the nature of reorientation processes and level crossing induced by elastic and inelastic collisions.

B. Fluorescence Detected Circular Dichroism (FDCD)

Tinoco and co-workers (University of California, Berkeley) have recently developed a novel method of measuring the circular dichroism (CD) of luminescent molecular species.¹¹⁹⁻¹²² The method is referred to as fluorescence detected circular dichroism (FDCD). In FDCD, the difference in absorption for left- and right-circularly polarized light (i.e., CD) is obtained by measuring the difference in (total) fluorescence intensity for left- and right-circularly polarized excitation. The differential circularly polarized excitation spectrum then mimics the CD spectrum. This method is based on the usually valid assumption that the excitation spectrum of a luminescent molecule or chromophore parallels its absorption spectrum. This assumption, of course, breaks down for systems in which energy transfer occurs between absorbing and emitting chromophores; but even in these cases FDCD retains some utility if appropriate models can be developed for treating the energy-transfer mechanisms and processes. By placing the luminescent sample in a magnetic field (*aligned parallel to the direction of excitation*), one may also measure fluorescence detected magnetic circular dichroism (FDMCD).¹²³

In the conventional FDCD experiment, the *total* luminescence intensity is measured without regard for polarization content. FDCD experiments may also be performed in which the lumi-

nescence is assayed for linearly polarized components or for the intensity ratios of (orthogonal) linearly polarized components. Tinoco et al.¹²² have shown that these latter experiments can provide very valuable and unique molecular structural information in cases where the optically active sample contains an orientationally nonisotropic distribution of excited (emitting) molecules due to photoselection and slow reorientational relaxation processes.

FDCD, like conventional CD spectroscopy, is a probe of molecular ground-state structural parameters (conformation, configuration, stereochemistry, etc.). In contradistinction, CPL is a probe of molecular excited (emitting) state structural features. Therefore, although the instrumentation and measurements techniques for FDCD and CPL have many features in common, these two spectroscopic methods probe different aspects of molecular structure. FDCD has enormous potential as a tool for studying molecular structure, and many of its applications have been described and discussed in a series of papers by Tinoco and his collaborators.¹¹⁹⁻¹²² Problems arising in the interpretation of FDCD data have also been discussed by White, Pao, and Tang¹²⁴ and by Ehrenberg and Steinberg.¹²⁵

VI. Summary

Circular polarization of molecular luminescence is a phenomenon of significant potential for exploitation as a probe of molecular stereochemistry and electronic structure. Natural CPL may be used to probe the stereochemical details of molecular emitting states just as CD is used to study ground-state molecular conformation and stereochemistry. Furthermore, the effects of photoselection and orientational relaxation upon CPL observables (such as ΔI and g_{lum}) may be used to evaluate molecular parameters (static and dynamic) not amenable to investigation by other spectroscopic techniques.^{14,15,27} The inherent sensitivity of emission measurement techniques affords the opportunity of using CPL and MCPL to probe excited (emitting) states not accessible by absorption (CD and MCD) techniques. Time-resolved CPL and MCPL measurements offer the additional possibility of studying molecular excited-state dynamics.

The general theory of molecular CPL and MCPL has been worked out;^{14,15,27} however, detailed models relating the CPL observables to specific molecular structural properties remain in a somewhat less developed state. Useful spectra-structure correlations have been achieved in a large number of cases, but these remain qualitative or semiquantitative rather than quantitative. The obstacles to further developments in spectra (CPL)-structure relationships are similar to those encountered in the use of CD and MCD as molecular structure probes.

The instrumentation required for performing "steady-state" CPL/MCPL measurements is simple in design and construction.^{9,20} High-sensitivity emission instrumentation may be readily modified or adapted for measuring the differential circular polarization of luminescence. Time-resolved CPL/MCPL measurements have not yet been reported. Such measurements present very difficult technical problems, but their potential value demands that they be attempted.

Further development of CPL spectroscopy as a probe of molecular structure will depend upon progress in the following areas: (a) development of detailed molecular theories (or models) relating CPL observables to specific molecular parameters, (b) improvement of CPL instrumentation and the capability of performing time-resolved measurements, (c) experimentation with various excitation-emission geometries and excitation polarizations, and (d) the extension of applications to a wider variety of luminescent systems.

VII. Appendix

Equation 68 gives the magnetic-field-induced CPL intensity (ΔI) for a $N \rightarrow S$ emission in terms of the Faraday \mathcal{A} , \mathcal{B} , and

\mathcal{C} parameters. Explicit expressions for the \mathcal{A} , \mathcal{B} , and \mathcal{C} parameters in the molecular coordinate system are given in this appendix, for the case of steady-state emission detection. Bars over the \mathcal{A} , \mathcal{B} , and \mathcal{C} parameters denote steady-state emission conditions. These expressions include only the electric dipole–electric dipole contributions to the transition probabilities (see ref 27 for higher order contributions). Furthermore, these expressions were derived based on the photoselection/reorientational relaxation model discussed in section II.B. The notation is that introduced in section II.B.

$$\Delta I = (1/2)\hbar\omega_{\ell}K(\omega_{\ell})N_{\mathcal{N}}^0\tau b_0\{\overline{\mathcal{A}}(\mathcal{N}\rightarrow\mathcal{G})f_{\text{MCPL}}^{\ell}(\omega)/\hbar + [\overline{\mathcal{B}}(\mathcal{N}\rightarrow\mathcal{G}) + \mathcal{C}(\mathcal{N}\rightarrow\mathcal{G})/kTf_{\text{MCPL}}^{\ell}(\omega)]\}$$

Isotropic (“Relaxed”) Limit: $D\tau \gg 1$

$$\overline{\mathcal{A}}(\mathcal{N}\rightarrow\mathcal{G}) = (-1/d_{\mathcal{N}})\sum_{g,n}(1/3)\text{Im}[\mu^{ng}\times\mu^{gn}\cdot(\mathbf{m}^{nn}-\mathbf{m}^{gg})] \quad (\text{A1})$$

$$\overline{\mathcal{B}}(\mathcal{N}\rightarrow\mathcal{G}) = (+1/d_{\mathcal{N}})\sum_{g,n}(1/3)\text{Im}\left\{\sum_{m\neq n}[\mu^{mg}\times\mu^{gn}\cdot\mathbf{m}^{mm} + \mu^{ng}\times\mu^{gm}\cdot\mathbf{m}^{mn}]/\Delta E_{nm} + \sum_{k\neq g}[\mu^{nk}\times\mu^{gn}\cdot\mathbf{m}^{kg} + \mu^{ng}\times\mu^{kn}\cdot\mathbf{m}^{gk}]/\Delta E_{gk}\right\} \quad (\text{A2})$$

$$\overline{\mathcal{C}}(\mathcal{N}\rightarrow\mathcal{G}) = (-1/d_{\mathcal{N}})\sum_{g,n}\text{Im}\{(1/3)\mu^{ng}\times\mu^{gn}\cdot\mathbf{m}^{nn}\} \quad (\text{A3})$$

Photoselected (“Frozen”) Limit: $D\tau \ll 1$

$$\overline{\mathcal{A}}(\mathcal{N}\rightarrow\mathcal{G}) = (+1/5d_{\mathcal{N}})\sum_{g,n}\text{Im}\{(1+2\sin^2\alpha\sin^2\beta)[\mu_y^{ng}\mu_x^{gn}\times(m_z^{nn}-m_z^{gg}) - \mu_x^{ng}\mu_y^{gn}(m_z^{nn}-m_z^{gg})] + (1+2\cos^2\alpha)\cdot\mu_x^{ng}\mu_z^{gn}(m_y^{nn}-m_y^{gg}) - \mu_y^{ng}\mu_z^{gn}(m_x^{nn}-m_x^{gg})\} + (1+2\sin^2\alpha\cos^2\beta)\cdot[\mu_z^{ng}\mu_y^{gn}(m_x^{nn}-m_x^{gg}) - \mu_z^{ng}\mu_x^{gn}(m_y^{nn}-m_y^{gg})]\} \quad (\text{A4})$$

$$\overline{\mathcal{B}}(\mathcal{N}\rightarrow\mathcal{G}) = (-1/5d_{\mathcal{N}})\sum_{g,n}\text{Im}\left\{\sum_{m\neq n}[(1+2\sin^2\alpha\sin^2\beta)\times(\mu_y^{mg}\mu_x^{gn}m_z^{nm} - \mu_x^{mg}\mu_y^{gn}m_z^{nm}) + (1+2\cos^2\alpha)(\mu_x^{mg}\mu_z^{gn}m_y^{nm} - \mu_y^{mg}\mu_z^{gn}m_x^{nm}) + (1+2\sin^2\alpha\cos^2\beta)(\mu_z^{mg}\mu_y^{gn}m_x^{nm} - \mu_z^{mg}\mu_x^{gn}m_y^{nm}) + (1+2\sin^2\alpha\sin^2\beta)\cdot(\mu_y^{ng}\mu_x^{gm}m_z^{mn} - \mu_x^{ng}\mu_y^{gm}m_z^{mn}) + (1+2\cos^2\alpha)(\mu_x^{ng}\mu_z^{gm}m_y^{mn} - \mu_y^{ng}\mu_z^{gm}m_x^{mn}) + (1+2\sin^2\alpha\cos^2\beta)(\mu_z^{ng}\mu_y^{gm}m_x^{mn} - \mu_z^{ng}\mu_x^{gm}m_y^{mn})]/\Delta E_{nm} + \sum_{k\neq g}[(1+2\sin^2\alpha\sin^2\beta)(\mu_y^{nk}\mu_x^{gn}m_z^{kg} - \mu_x^{nk}\mu_y^{gn}m_z^{kg}) + (1+2\cos^2\alpha)\cdot(\mu_x^{nk}\mu_z^{gn}m_y^{kg} - \mu_y^{nk}\mu_z^{gn}m_x^{kg}) + (1+2\sin^2\alpha\cos^2\beta)(\mu_z^{nk}\mu_y^{gn}m_x^{kg} - \mu_z^{nk}\mu_x^{gn}m_y^{kg}) + (1+2\sin^2\alpha\sin^2\beta)(\mu_y^{ng}\mu_x^{kn}m_z^{gk} - \mu_x^{ng}\mu_y^{kn}m_z^{gk}) + (1+2\cos^2\alpha)(\mu_x^{ng}\mu_z^{kn}m_y^{gk} - \mu_y^{ng}\mu_z^{kn}m_x^{gk}) + (1+2\sin^2\alpha\cos^2\beta)\cdot(\mu_z^{ng}\mu_y^{kn}m_x^{gk} - \mu_z^{ng}\mu_x^{kn}m_y^{gk})]/\Delta E_{gk}\right\} \quad (\text{A5})$$

$$\overline{\mathcal{C}}(\mathcal{N}\rightarrow\mathcal{G}) = (+1/5d_{\mathcal{N}})\sum_{g,n}\text{Im}\{(1+2\sin^2\alpha\sin^2\beta)\times(\mu_y^{ng}\mu_x^{gn}m_z^{nn} - \mu_x^{ng}\mu_y^{gn}m_z^{nn}) + (1+2\cos^2\alpha)(\mu_x^{ng}\mu_z^{gn}m_y^{nn} - \mu_y^{ng}\mu_z^{gn}m_x^{nn}) + (1+2\sin^2\alpha\cos^2\beta)(\mu_z^{ng}\mu_y^{gn}m_x^{nn} - \mu_z^{ng}\mu_x^{gn}m_y^{nn})\} \quad (\text{A6})$$

Note that eq A4, A5, and A6 reduce to the isotropic limit (given above) if $\beta = 90^\circ$ and $\alpha = 35.26^\circ$ (or 144.74°).

Acknowledgments. This work was supported by grants from the National Science Foundation and the Camille and Henry Dreyfus Foundation (through a Teacher-Scholar Award to F.R.). We are grateful for the contributions and help given by the following colleagues and collaborators (in CPL spectroscopy): Dr. Harry Brittain, Dr. James Demas, Dr. C. K. Luk, Dr. R. B. Martin, Dr. Paul Schatz, and Dr. Warren Yeakel. We also acknowledge helpful correspondence from Dr. Ignacio Tinoco (Berkeley) and Dr. Rodney Roche (University of Calgary). Special gratitude is expressed to Dr. Izchak Steinberg (Weizmann Institute, Israel) and Dr. John Schellman (University of Oregon) for their help and critical comments on various aspects of our work on circularly polarized luminescence spectroscopy.

IX. References

- J. A. Schellman, *Chem. Rev.*, **75**, 323 (1975).
- B. N. Samoilov, *J. Exp. Theor. Phys.*, **18**, 1030 (1948).
- M. S. Brodin and V. Reznichenko, *Ukr. Phys. J.*, **10**, 178 (1965).
- O. Neunhoeffer and H. Ulrich, *Z. Elektrochem.*, **59**, 122 (1955).
- C. H. Emeis and L. J. Oosterhoff, *Chem. Phys. Lett.*, **1**, 129, 268 (1967).
- C. A. Emeis, Ph.D. Thesis, The University of Leiden, The Netherlands, 1968.
- C. A. Emeis and L. J. Oosterhoff, *J. Chem. Phys.*, **54**, 4809 (1971).
- H. P. J. M. Dekkers, C. A. Emeis, and L. J. Oosterhoff, *J. Am. Chem. Soc.*, **91**, 4589 (1969).
- I. Steinberg and A. Gafni, *Rev. Sci. Instrum.*, **43**, 409 (1972).
- C. K. Luk and F. S. Richardson, *J. Am. Chem. Soc.*, **96**, 2006 (1974).
- C. K. Luk and F. S. Richardson, *J. Am. Chem. Soc.*, **97**, 6666 (1975).
- I. Steinberg in "Biochemical Fluorescence: Concepts", Vol. I. R. F. Chen and H. Edelhoch, Ed., Marcel-Dekker, New York, N.Y., 1975, Chapter 3.
- J. Snir and J. A. Schellman, *J. Phys. Chem.*, **78**, 387 (1974).
- I. Steinberg and B. Ehrenberg, *J. Chem. Phys.*, **61**, 3382 (1974).
- J. P. Riehl and F. S. Richardson, *J. Chem. Phys.*, **65**, 1011 (1976).
- R. A. Shatwell and A. J. McCaffery, *Chem. Commun.*, 546 (1973).
- A. J. McCaffery, P. Brint, R. Gale, and R. A. Shatwell, *Chem. Phys. Lett.*, **22**, 600 (1973).
- R. A. Shatwell, R. Gale, A. J. McCaffery, and K. Sichel, *J. Am. Chem. Soc.*, **97**, 7015 (1975).
- R. A. Shatwell and A. J. McCaffery, *Mol. Phys.*, **30**, 1489 (1975).
- R. A. Shatwell and A. J. McCaffery, *J. Phys. E*, **7**, 297 (1974).
- C. K. Luk, W. C. Yeakel, F. S. Richardson, and P. N. Schatz, *Chem. Phys. Lett.*, **34**, 147 (1975).
- H. G. Brittain, F. S. Richardson, J. Jasinski, W. C. Yeakel, and P. N. Schatz, *Mol. Phys.*, **32**, 1751 (1976).
- W. C. Yeakel, R. W. Schwartz, H. G. Brittain, J. L. Slater, and P. N. Schatz, *Mol. Phys.*, **32**, 1751 (1976).
- N. Moreau, A. C. Boccardo, and J. Badoz, *Phys. Rev. B*, **10**, 64 (1974).
- K. W. Hipps, Ph.D. Dissertation, Washington State University, Pullman, Washington, 1976.
- A. Schreiner, private communication.
- J. P. Riehl and F. S. Richardson, *J. Chem. Phys.*, **66**, 1988 (1977).
- P. J. Stephens, *J. Chem. Phys.*, **52**, 3489 (1970).
- E. A. Power and R. Shail, *Proc. Cambridge Philos. Soc.*, **55**, 87 (1959).
- E. A. Power and S. Zienau, *Phil. Trans. R. Soc. (London)*, **A251**, 427 (1959).
- M. Babiker, E. A. Power, and T. Thirunamachandran, *Proc. R. Soc. London, Ser. A*, **338**, 235 (1974).
- P. W. Atkins and R. G. Wooley, *Proc. R. Soc. London, Ser. A*, **321**, 549 (1970).
- R. G. Wooley, *Adv. Chem. Phys.*, **33**, 153 (1975).
- W. P. Healy, *J. Chem. Phys.*, **64**, 3111 (1976).
- B. U. Felderhof, *Physica*, **71**, 557 (1971).
- E. A. Power and T. Thirunamachandran, *J. Chem. Phys.*, **60**, 3695 (1974).
- E. A. Power, "Introductory Quantum Electrodynamics", Longmans, London, 1964.
- G. Weber, *Biochem. J.*, **51**, 145 (1952).
- L. D. Favro, *Phys. Rev.*, **119**, 53 (1960).
- T. Tao, *Biopolymers*, **8**, 609 (1969).
- R. G. Gordon, *J. Chem. Phys.*, **45**, 1643 (1966).
- P. Wahl in ref 12, Chapter 1.
- F. Dorr in "Creation and Detection of the Excited State", Vol. I, Part A, A. A. Lamola, Ed., Marcel-Dekker, New York, N.Y., 1971, Chapter 2.
- I. Tinoco, B. Ehrenberg, and I. Z. Steinberg, *J. Chem. Phys.*, **66**, 916 (1977).
- H. P. J. M. Dekkers and L. E. Closs, *J. Am. Chem. Soc.*, **98**, 2210 (1976).
- S. N. Jasperson and S. E. Schnatterly, *Rev. Sci. Instrum.*, **40**, 761 (1969).
- J. I. Treu, A. B. Callender, and S. E. Schnatterly, *Rev. Sci. Instrum.*, **44**, 793 (1973).
- M. Billardon and J. Badoz, *C. R. Acad. Sci.*, **263**, 139 (1966).
- W. Johnson, Jr., *Rev. Sci. Instrum.*, **42**, 1283 (1971).
- G. A. Osborne, J. C. Cheng, and P. J. Stephens, *Rev. Sci. Instrum.*, **44**, 10 (1973).
- O. Schnepp, S. Allen, and E. F. Peason, *Rev. Sci. Instrum.*, **41**, 1136 (1970).
- G. Chabay and G. Holzwarth, *Appl. Opt.*, **14**, 454 (1975).

- (53) F. A. Ferrone, J. J. Hopfield, and S. E. Schnatterly, *Rev. Sci. Instrum.*, **45**, 1392 (1974).
- (54) M. Anson and P. M. Bayley, *J. Phys. E*, **7**, 1304 (1974).
- (55) M. F. Russel, M. Billardon, and J. P. Badoz, *Appl. Opt.*, **11**, 2375 (1972).
- (56) P. J. Stephens, *Annu. Rev. Phys. Chem.*, **25**, 201 (1974).
- (57) J. Wampler and R. J. DeSa, *Anal. Chem.*, **46**, 563 (1974).
- (58) L. I. Katzin, *Inorg. Chem.*, **7**, 1183 (1968).
- (59) L. I. Katzin, *Inorg. Chem.*, **8**, 1649 (1969).
- (60) L. I. Katzin and E. Gulyas, *Inorg. Chem.*, **7**, 2442 (1968).
- (61) R. Prados, L. G. Stadtherr, H. Donato, and R. B. Martin, *J. Inorg. Nucl. Chem.*, **36**, 689 (1974).
- (62) S. Misumi, S. Kida, and T. Isobe, *Spectrochim. Acta, Part A*, **24**, 271 (1968).
- (63) S. Misumi, T. Isobe, and H. Furuta, *Bull. Chem. Soc. Jpn.*, **47**, 421 (1974).
- (64) S. Misumi, S. Kida, T. Isobe, Y. Nishida, and H. Furuta, *Bull. Chem. Soc. Jpn.*, **42**, 3433 (1969).
- (65) B. Norden and I. Grerthe, *Acta Chem. Scand.*, **26**, 407 (1972).
- (66) N. H. Andersen, B. J. Bottino, A. Moore, and J. R. Shaw, *J. Am. Chem. Soc.*, **96**, 603 (1974).
- (67) J. Dillon and K. Nakanishi, *J. Am. Chem. Soc.*, **96**, 4057 (1974); **97**, 5417 (1975).
- (68) C. K. Luk and F. S. Richardson, *Chem. Phys. Lett.*, **25**, 215 (1974).
- (69) H. G. Brittain and F. S. Richardson, *Inorg. Chem.*, **15**, 1507 (1976).
- (70) H. G. Brittain and F. S. Richardson, *J. Am. Chem. Soc.*, **98**, 5858 (1976).
- (71) H. G. Brittain and F. S. Richardson, *J. Chem. Soc., Dalton Trans.*, 2253 (1976).
- (72) H. G. Brittain and F. S. Richardson, *J. Am. Chem. Soc.*, **99**, 65 (1977).
- (73) H. G. Brittain and F. S. Richardson, *Bioinorg. Chem.*, **7**, 233 (1977).
- (74) G. Hilmes, H. G. Brittain, and F. S. Richardson, *Inorg. Chem.*, **16**, 528 (1977).
- (75) See, for example, (a) G. W. Robinson, *Can. J. Phys.*, **34**, 699 (1956); (b) J. C. D. Brand, *J. Chem. Soc.*, 858 (1956); (c) J. R. Henderson and M. Muramoto, *J. Chem. Phys.*, **43**, 1215 (1965).
- (76) V. T. Jones and J. B. Coon, *J. Mol. Spectrosc.*, **31**, 137 (1969).
- (77) H. G. Brittain and F. S. Richardson, *J. Phys. Chem.*, **80**, 2590 (1976).
- (78) A. Gafni and I. Steinberg, *Photochem. Photobiol.*, **15**, 93 (1972).
- (79) J. Schlessinger and A. Warshel, *Chem. Phys. Lett.*, **28**, 380 (1974).
- (80) J. Schlessinger, A. Gafni, and I. Z. Steinberg, *J. Am. Chem. Soc.*, **96**, 7396 (1974).
- (81) Y. Shindo and T. Miura, *J. Phys. Chem.*, **77**, 1817 (1973).
- (82) J. Schlessinger and I. Z. Steinberg, *Proc. Natl. Acad. Sci. U.S.A.*, **69**, 769 (1972).
- (83) A. Gafni, J. Schlessinger, and I. Z. Steinberg, *Isr. J. Chem.*, **11**, 423 (1973).
- (84) S. Veinberg, S. Shaltiel, and I. Z. Steinberg, *Isr. J. Chem.*, **12**, 421 (1974).
- (85) J. Schlessinger and A. Levitzki, *J. Mol. Biol.*, **82**, 547 (1974).
- (86) J. Schlessinger, I. Z. Steinberg, and I. Pecht, *J. Mol. Biol.*, **87**, 725 (1974).
- (87) A. Gafni and I. Z. Steinberg, *Biochemistry*, **13**, 800 (1974).
- (88) J. Schlessinger, I. Z. Steinberg, and A. Levitzki, *J. Mol. Biol.*, **91**, 523 (1975).
- (89) J. Schlessinger, R. S. Roche, and I. Z. Steinberg, *Biochemistry*, **14**, 255 (1975).
- (90) I. Z. Steinberg, J. Schlessinger, and A. Gafni in "Peptides, Polypeptides, and Proteins", E. R. Blout, F. A. Bovey, M. Goodman, and N. Lotan, Ed., Wiley, New York, N.Y., 1974, pp 351-369.
- (91) A. Grinvald, J. Schlessinger, I. Pecht, and I. Z. Steinberg, *Biochemistry*, **14**, 1921 (1975).
- (92) J. Schlessinger, I. Z. Steinberg, D. Givol, and J. Hochman, *FEBS Lett.*, **52**, 231 (1975).
- (93) J. C. Jaton, H. Huser, D. G. Braun, D. Gival, I. Pecht, and J. Schlessinger, *Biochemistry*, **14**, 5312 (1975).
- (94) D. Givol, I. Pecht, J. Hochmann, J. Schlessinger, and I. Z. Steinberg, *Proc. Int. Congr. Immunol.*, **2nd**, 1, 39 (1974).
- (95) J. Schlessinger, I. Z. Steinberg, D. Givol, J. Hochmann, and I. Pecht, *Proc. Natl. Acad. Sci. U.S.A.*, **72**, 2775 (1975).
- (96) A. Gafni, H. Hardt, and I. Z. Steinberg, *Biochim. Biophys. Acta*, **387**, 256 (1975).
- (97) W. F. Riesen, J. Schlessinger, and J.-C. Jaton, *Biochemistry*, **15**, 3391 (1976).
- (98) H. G. Brittain, F. S. Richardson, and R. B. Martin, *J. Am. Chem. Soc.*, **98**, 8255 (1976).
- (99) H. G. Brittain, F. S. Richardson, R. B. Martin, L. Burntack, and C. Kay, *Biochem. Biophys. Res. Commun.*, **68**, 1013 (1976).
- (100) T. L. Miller, D. J. Nelson, H. G. Brittain, F. S. Richardson, R. B. Martin, and C. Kay, *FEBS Lett.*, **58**, 262 (1975).
- (101) H. Donato and R. B. Martin, *Biochemistry*, **13**, 4575 (1974).
- (102) D. J. Nelson, T. L. Miller, and R. B. Martin, *Bioinorg. Chem.*, in press.
- (103) Dr. Rodney Roche, private communication.
- (104) M. Epstein, Ph.D. Thesis, The Weizmann Institute of Science, Rehovot, Israel, 1976.
- (105) H. G. Brittain and F. S. Richardson, unpublished results.
- (106) W. C. Yeakel, *Mol. Phys.*, **33**, 1429 (1977).
- (107) A. J. McCaffery and R. Shatwell, *Phys. Rev. B*, **12**, 3815 (1975).
- (108) A. J. McCaffery in "Electronic States of Inorganic Compounds: New Experimental Techniques", P. Day, Ed., D. Reidel Publishing Co., Dordrecht-Holland, 1975.
- (109) R. A. Shatwell and A. J. McCaffery, *Chem. Phys. Lett.*, **32**, 430 (1975).
- (110) R. W. Schwartz, H. G. Brittain, J. P. Riehl, W. C. Yeakel, and F. S. Richardson, *Mol. Phys.*, **34**, 361 (1977).
- (111) R. W. Schwartz, J. P. Riehl, H. G. Brittain, E. Krausz, and F. S. Richardson, unpublished results.
- (112) F. S. Richardson and H. G. Brittain, unpublished results.
- (113) M. J. Marrone and M. N. Kabler, *Phys. Rev. Lett.*, **27**, 1283 (1971).
- (114) J. Vigue, M. Broeyer, and J. C. Lehmann, *J. Chem. Phys.*, **62**, 4941 (1975).
- (115) P. P. Feofilov, "The Physical Basis of Polarized Emission", Consultants Bureau, New York, N.Y., 1961.
- (116) R. Clark, S. R. Jeyes, A. J. McCaffery, and R. A. Shatwell, *Chem. Phys. Lett.*, **25**, 74 (1974).
- (117) R. Clark and A. J. McCaffery, *J. Chem. Soc., Chem. Commun.*, 1039 (1974).
- (118) H. Kato, R. Clark, and A. J. McCaffery, *Mol. Phys.*, **31**, 943 (1976).
- (119) D. H. Turner, I. Tinoco, and M. Maestre, *J. Am. Chem. Soc.*, **96**, 4340 (1974).
- (120) D. H. Turner, I. Tinoco, and M. Maestre, *Biochemistry*, **14**, 3794 (1975).
- (121) I. Tinoco and D. H. Turner, *J. Am. Chem. Soc.*, **98**, 6453 (1976).
- (122) I. Tinoco, B. Ehrenberg, and I. Z. Steinberg, *J. Chem. Phys.*, in press.
- (123) J. C. Sutherland and H. Low, *Proc. Natl. Acad. Sci. U.S.A.*, **73**, 726 (1976).
- (124) T. G. White, Y.-H. Pao, and M. M. Tang, *J. Am. Chem. Soc.*, **97**, 4751 (1975).
- (125) B. Ehrenberg and I. Z. Steinberg, *J. Am. Chem. Soc.*, **98**, 1293 (1976).